Republic of Iraq

Ministry of Higher Education and

Scientific Research

Babylon University

College of Engineering

Automated Brain Tumor Detection and Segmentation Based on Magnetic Resonance Images

A thesis

Submitted to the College of Engineering\ University of

Babylon as Partial Fulfillment of the Requirements for the

Degree of Master in Engineering /Electrical engineering/ Indusdtial Electronic

By

Rasha Turki Khilkhal

Supervised

Asst.Prof.Dr. Mustafa Rashid Ismael

2023 A.D ***1444 A.H***

بسم الله الرحمن الرحيم

﴿ نَرْفَعُ دَرَجَاتٍ مَنْ نَشَاءُ وَفَوْقَ كُلِّ ذِي عِلْمٍ عَلِيمٌ ﴾

صدق الله العلي العظيم

سورة يوسف/ الآية (76)

Examining committee certificate

We certify that we have read this thesis entitled "**An Improved Method for Brain Tumor Detection and Segmentation in Magnetic Resonance Images"** and as an examining committee, examined the student **Rasha Turki Khilkhal** in its content and that in our opinion it meets the standard of a thesis for the degree of master in engineering/electrical engineering / Industrial Electronic.

Signature:	Signature:	Signature:
Name: Prof.	Name: Prof.	Name: Asst. Prof.
Dr.Saad Saffah Hasson	Dr. Qais Kareem Omran	Dr.Hussain Kareem Khleef
(chirman)	(member)	(member)
Date: / /2022	Date: / /2022	Date: / /2022

Signature:	Signature:
Name:	Name: Asst. Prof.
Dr. Mustafa Rashid	Dr. Shamam Fadhil Alwash
(supervisor)	(Head of Electrical Department)
Date: / /2022	Date: / /2022

Signature:

Name: Prof.

Dr. Hatem Hadi Obeid

(Dean of College of Engineering)

Date: / /2022

Supervisor certification

I certify that this thesis entitled ‘’ **An Improved Method for Brain Tumor Detection and Segmentation in Magnetic Resonance Images”** was prepared by **Rasha Turki** under my supervision at the department of electrical engineering, college of engineering, university of Babylon, as partial fulfillment of the requirements for the degree of master in engineering /electrical engineering /Industrial Electronic

Supervisor

Signature:

Name**: Dr. Mustafa Rashid**

Date: / /2022

In view of the above recommendation, I forwarding this thesis for discussion by the Examination Committee.

Head of Electrical Department

Signature:

Name: Asst. Prof .Dr. Shamam Fadhil Alwash

Date: / / 2022

Acknowledgments

First and foremost, I praise and thank my God "ALLAH", the Almighty, for blessing me to complete this work successfully despite all the difficulties.

I would like to give a strong thanks to my parents, for supporting me spiritually throughout my life, sisters, and brothers who along the way believed in me.

I would like to express my deepest sincere gratitude to my advisor Dr. Mustafa Rashid for the continuous support of my thesis, their sharp and quick understanding of the issues, and their advice which made me learn much. in addition, their patience, enthusiasm, motivation, and guidance helped me in all the time of this thesis also they have taught me the methodology to present this thesis as clearly as possible.

My thanks also go to all the people who work within the Department of Electrical Engineering /College of Engineering/University of Babylon/Iraq for their help in many matters

Rasha Turki

Abstract

Brain tumors are fatal diseases because they have a low survival rate. In order to provide effective treatment for brain tumors, an accurate diagnosis is required. In medical image processing, the detection and segmentation of brain tumors utilizing magnetic resonance imaging (MRI) is a crucial step. This results from the beneficial information obtained from MRI images that help the radiologist in brain diagnosis. The manual detection and segmentation of the tumor region from MRI slices is a sophisticated, time-consuming process, especially when dealing with a large number of MRI Images. Therefore, an efficient and reliable detection model is required.

In this work, an automated diagnosis method is proposed that comprises two main steps; detection of tumor slice and segmentation of tumor region in the detected slice. In the detection step, machine learning was utilized to detect and classify the brain MRI. Features are extracted from each MRI slice using Histogram of Oriented Gradient (HOG), then these slices are classified into the tumor and non-tumor images using three types of classifier models, k-Nearest Neighbor (KNN), Support Vector Machine (SVM) and Artificial Neural Network (ANN). ANN algorithm with a 99.7 % accuracy rate was found to be better compared to other algorithms at ratio (80%,10%,10%).

On the other hand, K-means clustering, thresholding, and morphological operations methods are implemented in the segmentation step. The median filter is used to enhance the quality of the MRI slices and improve the segmentation performance by reducing the noise level. Four morphological operations have demonstrated significant improvements in the segmentation process, erosion, dilation, closing, and opening. The

simulation ware applied on two datasets, Kaggle which consists of (3000) images, and BRATS (high-grade (HGG) and low-grade (LGG) images).

The results obtained from the simulation demonstrated the powerful achievements of the suggested algorithm in terms of accuracy was 99.7%, sensitivity was 99.4%, specificity was 99.5%, Dice ware 93.68% for LGG and 96.79% for HGG, Jaccard was 93.6, and F1 score was 96.8.

LIST OF CONTENTS

LIST OF FIGURE

LIST OF TABLE

LIST OF ACRONYMS

ANN	Artificial Neural Network
BRATS/BraTS	Brain tumor Segmentation
CNN	Convolutional Neural Network
CT	Computed Tomography
DWT	Discrete Wavelet Transform
FPR	False Positive Rate
FNR	False Negative Rate
FCM	Fuzzy C Means
FLAIR	Fluid Attenuated Inversion Recovery
FCM	Fuzzy C-Means clustering
GLCM	Gray Level Co-occurrence Matrix
HOG	Histogram of Oriented Gradient
HGG	High-grade Glioma
kNN	k Nearest Neighbor
LGG	Low-grade Glioma
MRI	Magnetic Resonance Imaging
ML	Machine Learning
ROC	Receiver Operating Characteristic
ROI	region of interest
SVM	Support Vector Machine
T1	longitudinal relaxation time
T2	transverse relaxation time
T1c	longitudinal relaxation time with contrast
TC	Tumor Core
TPR	True Positive Rate
TNR	Tue Negative Rate

Chapter one

Introduction

Chapter One

Introduction

1.1 Overview

The brain is made up of billions of nerves that process data simultaneously throughout our bodies. Gray and white material are the two primary elements of the brain, and they are arranged in different layers; the gray matter is made up of nerve cells in the brain known as neurons[1]. The white matter is made up of glial cells. The skull bones and a covering of three thin membranes called meninges protect the brain. The cerebrum, cerebellum, and brain stem are the three major parts of the brain [2]. Brain tumors may develop inside the brain, on its surface, in the base-of-the-brain nerves, or outside the brain [3].

1.2 Types of brain tumors:

The brain tumor can be benign (non-cancerous), pre-malignant, or malignant (cancerous). A benign tumor is one that does not grow rapidly, does not have an effect on nearby healthy tissues, and does not spread to neighboring tissues. Premalignant Tumor is a precancerous stage that is considered a disease and Premalignant Tumor is a disease-causing precancerous stage and if left untreated, can lead to cancer. Malignancy (It consists of two syllables "mal-" which is Greek for "bad", and "ignis", which is Greek for "fire") refers to a type of tumor that exacerbates over time and finally kills a person. A malignant disease is one that is rapidly progressing and it is a common term used to describe cancer [4].

1.2.1. Primary brain tumor: An initial an unusual expansion that originates in the brain and typically does not spread to other areas of the skin

is referred to as a brain tumor. Both cancerous and benign astrocytomas are both possible [5].

1.2.2. Secondary (Metastatic) Brain tumors: Develop from their origins in other parts of the body. They develop as cancer cells move throughout the bloodstream. lung and breast malignancies are the most typical cancers that move to the brain [5].

The best method for finding brain tumors is (MRI). The scans produce enormous amounts of image data. These images are examined by a radiologist. Because of the complexities of brain tumors and their characteristics, a manual investigation can be error-prone.

1.3 Detection and Segmentation

Tumor detection in the brain tumor diagnosis center is still carried out manually. Detecting tumors in MRI reports, according to the radiologist, takes a long time, a single report takes about ten to fifteen minutes to diagnose. Tumor detection differs from expert to expert as well. Current technology necessitates precise tumor extraction in much less time [11]. In this case, a computer-controlled tumor detection method should classify MR images as normal or tumors faster and more accurately [12]. It should be coherent and provide radiologists with a self-explanatory and straightforward system. This is possible by combining the segmentation method with previous knowledge of tissue intensity as well as other characteristics like shape, size, symmetry, and anatomical and functional variability. Tumor detection and segmentation by machine assistance in surgical treatment development and review. On the other hand, as the impact of machine learning grows in our lives and society, artificial intelligence may begin to play an important role in medical diagnosis and the support of doctors and surgeons. Ml Algorithms are most commonly used to analyze

medical images in order to identify, distinguish, and classify brain tumors into subheadings, allowing professionals to make a diagnosis [6].

The basic function of segmentation is to easily extract information and various features from images. Methods for segmenting brain tumors can be divided into three categories based on the amount of human interaction required [7]: Segmentation can be carried out manually, semi-automatically, or fully automatically [16]. Manual segmentation is carried out by humans (radiologists/anatomists/trained technologists) who use not just the data contained in the image but also gain more knowledge such as physiology. To make drawing regions of interest and displaying images easier, Manual delineation necessarily requires the utilization of software applications with advanced graphical interfaces. In practice, selecting the region of interest (ROI), is a time-consuming and tedious task [8]. In semi-automatic brain tumor segmentation, it is frequently necessary to use a human operator to set up the process, check the results' accuracy or even manually fix the segmentation outcome. Most recent studies focus on the semi-automatic segmentation of brain tumors that requires as little human interaction as possible [9]. Tumor segmentation is decided by the computer using fully automatic methods with no human involvement. Because it is a problem that people can effectively learn to solve, the study of automatic brain tumor segmentation makes for an intriguing research topic. On the other hand, it's still challenging to create highly accurate automated methods [10].

1.4 Literature Survey

It is essential to create an automated system for analyzing MRI data and segmenting brain tumors to lessen workload and human error. However, it is still a difficult task. Over the past few decades, numerous studies and approaches have been reported and suggested to address this issue.

Reviewing the most recent related works is necessary in order to study the detection and segmentation of brain tumors.

A. A. Padmanabha G, et al. 2017 [11] proposed a method for detecting brain tumors by combining (Discrete Wavelet Transform (DWT), GLCM, LBP, and HOG) methods to extract features from MRI and classify it by using ML techniques to achieve the high accuracy.

M. R. Islam, et.al 2018 [12] proposed a method for detecting brain tumors by combining thresholding method and morphological algorithm processes with HOG features to identification of brain tumors. This method is only appropriate for images that are less noisy and self-evident. When compared to earlier research, the best accuracy was also enhanced.

D. Reddy, et.al 2018 [13] proposed a method for segmenting brain tumors, that is automated to prevent noise creation, the median filter was utilized to preprocess the MRI. K-Means Clustering and Threshold have been employed to segment the images during the segmentation phase.

A. Wadhwa, et al. 2019 [14] worked on a comparative analysis of brain tumor detection from MRI data utilizing (k-means), (fuzzy c-means), and (hierarchical) clustering algorithms.

M. Gurbina et al. 2019 [15] investigated some types of brain tumors, including metastatic bronchogenic squamous cell tumors, gliomas, and sarcoma, using brain magnetic resonance (MRI), and suggested a system for detecting and classifying MRI brain tumors using various wavelet transforms and SVM.

C. Zhang et al 2019 [16] suggested a brain tumor segmentation system. To begin, adaptive Wiener filtering can be used for noise removal, and morphological operations are used to expose cells, trying to lower the

method's noise sensitivity. Second, K-means++ clustering is used in conjunction with the Gaussian kernel-based fuzzy C-means algorithm to segment images.

J. Amin, et al. 2020 [17] developed an automated methodology for early detection of brain tumors and classified the tumors into 2 classifications Following segmentation of the tumors, shape, and density features were derived. The author employed the SVM classifier, which yielded 97.1 percent accuracy, 98.00 percent specificity, and 91.90 percent sensitivity. This technique identified the tumor more precisely because it took less time to execute.

T. Saba, et al. 2020 [18] proposed trying to combine HOG (Histogram of Gradient) and LBP (Local Binary Pattern) features to discover tumors in brain MRI Prior to actually classification, before classifying the data, they combined the textural feature with the refined transfer learning features and employed an entropy-based feature optimization algorithm.

M. Rashid Ismael 2021 [19] proposed an automated method for creating an active contour model using edge sharpening, thresholding, and morphological operations. In the sharpening process, four edge detection methods (Sobel, Roberts, Prewitt, and Canny) are used, and their performance is evaluated using Dice, Jaccard, and F1 scores.

S. Deepak et. al. 2021 [20] Proposed multiclass SVM is suggested used with CNN features. The embedded framework was analyzed and validated using a five-fold cross-validation procedure. Overall, the suggested framework had a classification accuracy of 95.82 percent. Whenever the amount of available training data is limited, the SVM classifier model outperformed the soft-max classifier for CNN features. In comparison to

transfer learning-based classification, the CNN-SVM strategy requires fewer mathematical calculations and memory.

R. Mostafiz et. al. 2021 [21] proposed a good tumor identification scheme based on the combination of HOG gradients and deep CNN neural features from MRI.

D. M. Toufiq et al. 2022 [22] Suggested an Optimization method threshold difference technique has two stages: the first is skull identifying and brain geographic area segmentation to enhance the segmentation process, and the second is segmentation. Due to the close proximity of the impacted regions in the MRI images, it has been suggested to segment the portion of the brain and differentiate it from the skull. The second step is used to segment the tumor from the central nervous system region image in two levels: first, a layer image is generated, and then the threshold distinction process is tried to apply between the segmented brain MRI images and the layer image. The Gray Level Co-occurrence Matrix yielded a set of eight textural features. RST was then employed to completely disregard the features that resulted in a false prediction. Eventually, the classification is carried out using ID3. accomplished a 90% success rate.

H. Habib et.al 2022 [23] proposed an algorithm for automated segmentation and classification. This research attempts to segment brain tumors from Image data utilizing threshold segmentation and the watershed method, and then classify brain tumors based on selected features (MSER, FAST, and so on) using various classifiers.

S. Rinesh, et.al 2022 [24] proposed a method for tumor position in the brain using multiple operations on hyperspectral images. Melding k-based clustering procedures such as k-means clustering and k-nearest neighboring yields the tumor. The optimal control processes eliminate the need for

computation to determine the best value of K for brain region segmentation. The accuracy, sensitivity, and specificity of their proposed model were lower than those of our techniques at 96.47%, 96.32%, and 98.24%, respectively.

M. T. Nyo,et al. 2022 [25] proposed a method for segmenting brain tumors that is automated. In the pre-processing stage, MR images are transformed into gray images and resized to the exact same volume. In addition, a median filter is developed to remove noise from MR images. The various classes of Otsu's thresholding are utilized to segment the brain tumor. The morphological operation was then used to obtain the precise tumor area. The research is all run on the 2015 BRATS dataset. The Jaccard index, Sensitivity, Specificity, and accuracy were used as segmentation quality validation metrics. The results show accuracy of 95.55%.

According to the findings of the preceding study, there are three major issues in brain tumor research: (a) MR image area segmentation, (b) retrieval of advanced features, and (c) a strategy for detection or classification based on features that were extracted.

1.5 Problem Statement:

Researchers have proposed several region clustering algorithms, however the optimal one must be identified. In contrast, there are several ways for extracting characteristics that are founded on just one approach or a combination of two approaches. The fusion process produces superior outcomes in general. Finally, because of the quantity of available algorithms, selecting a decent detection algorithm is challenging. For the reasons indicated above, we are motivated to work on these challenges in order to establish a solid overall system.

Throughout this work, the Histogram of Oriented Gradient (HOG) is used to extract features from medical images of patients' tumors in the data

set, and these images are then classified as a tumor or non-tumor images using (KNN), (SVM), and (ANN). which produces more precise results. Brain tumor image segmentation was used after detection. Automated system for segmenting brain tumors based on k-means clustering, thresholding, and morphological operations. K-means first divides the MRI slice into three parts, and then a thresholding stage converts the segmented image to black and white to distinguish the tumor from non-tumor areas. K-means is used as an intermediate stage before thresholding to improve the segmentation process's performance. On the other hand, non-brain tissue is removed utilizing morphological operations. Four morphological operations have demonstrated significant improvements in the process suggested in this method, erosion, dilation, closing, and opening. The experiments were implemented on BRATS datasets utilizing high-grade (HGG) and low-grade (LGG) images.

1.6 Aim and Objective

The aims of this work are summarized as follows:

1. Design and simulation a brain tumor detection and classification system that helps the radiologist in brain diagnosis essential to ensure early detection and categorization of Tumor.
2. Detect the presence of a tumor in brain images and classify the tumors and non-tumors correctly.
3. Segment the tumor region from the brain MRI.

1.7 Thesis Organization

The five chapters that make up this thesis

Chapter One: Which include the general introduction of Brain tumors types, the basic concept of Magnetic Resonance Image (MRI) scan,

Detection and Segmentation of brain tumors, literature survey, and aims of the work.

Chapter two: Provides the background of brain tumor detection, classification, segmentation, and machine learning algorithms that have been applied in this field and how these technologies have been grown in recent years.

Chapter Three: Introduces the proposed techniques of Brain tumor detection and segmentation.

Chapter Four: Shows the results and discussion of the proposed techniques.

Chapter Five: Presents the conclusions of the thesis and their future works.

Chapter two

Theories and methods

Chapter Two

Theories and Methods

2.1. Introduction:

The possibility of radiologists misdiagnosing a patient exists when a large volume of MRI data needs to be analyzed because the human eye loses sensitivity as more cases are encountered, typically when only a few slices are impacted. In order to analyze and categorize medical images, effective automated systems are therefore required. Both typical and abnormal images may be present in the MRI [5].

CT, PET, and MRI are common medical imaging methods. The most popular of these is MRI. It is highly sensitive to local changes in tissue water, which reflect physiologic changes that can be seen by MRI, which is one reason for this. In contrast to other medical imaging methods, enables the high-resolution differentiation of soft tissues. Using different image acquisition techniques and variables, MRI can produce multiple images of the same tissue with a variety of contrast visualization. Within the same tissue, these additional MR images offer helpful biological data. By combining information from various contrast mechanisms, more in-depth research is being done on brain pathology.

This chapter provides an overview of existing methods for analyzing brain tumors on MRI. Furthermore, the chapter provides the statement of the problem, goals, and conceptual framework of the study to address the difficult issues that these methods present. These methods are designed for tumor detection, classification, and segmentation in order to provide the radiologist with comprehensive assistance in tumor diagnosis. Tumor detection identifies the cancer-affected area on a medical image, while tumor classification defines the type of segmented tumor[26].

2.2. Detection

The detection of a tumor on an MRI image is difficult because the image contains other organs or tissues adjoining the tumor. In medical images, a few of the organs are very close together and have similar levels of intensity. In such cases, segmenting the tumor has become difficult because the organ must be extracted first, followed by the tumor. To appropriately delineate the tumor area on a medical image, one must first understand the characteristics of a medical image, the anatomy of the organ, and the distinction between both normal and abnormal tissues [27].

2.2.1.Machine Learning (ML)

Machine Learning is one of the branches of artificial intelligence concerned with developing the algorithms, applications, and frameworks required to enable computers to learn by achieving more precise predictions and valuable results from the analysis of input data. Data mining is the application of machine learning algorithms to large databases. Machine learning, or ML, is also used to solve a variety of problems in speech recognition and robotics. Because the basic task of ML is an inference from a sample, the statistical theory has been used to construct mathematical models in machine learning. The role of ML is twofold. First, during training, an efficient algorithm is used to optimize a problem as well as store and process its data. Second, the model is only learned once. The inference representation and algorithmic solution must be effective [28]. The complexity of an algorithm, which is the mean space and time, is used to determine its predictive accuracy. Supervised Learning, Unsupervised Learning, and Reinforcement Learning are the three types of machine learning algorithms. In supervised learning, input and output must exist, as well as prediction accuracy during algorithm training. In the case of unsupervised learning, the training algorithm does not require any output. In

other words, unsupervised learning relies solely on input data. To monitor the complex learning system, supervised algorithms are used [6]. Reinforcement learning is distinct from supervised learning in that it does not call for the display of labelled input/output pairs or the explicit correction of suboptimal actions. Instead, the focus is on striking a balance between exploration (of previously unexplored territory) and exploitation (of current knowledge)[29]. The main Machin learning methods are depicted in Figure (2.1).

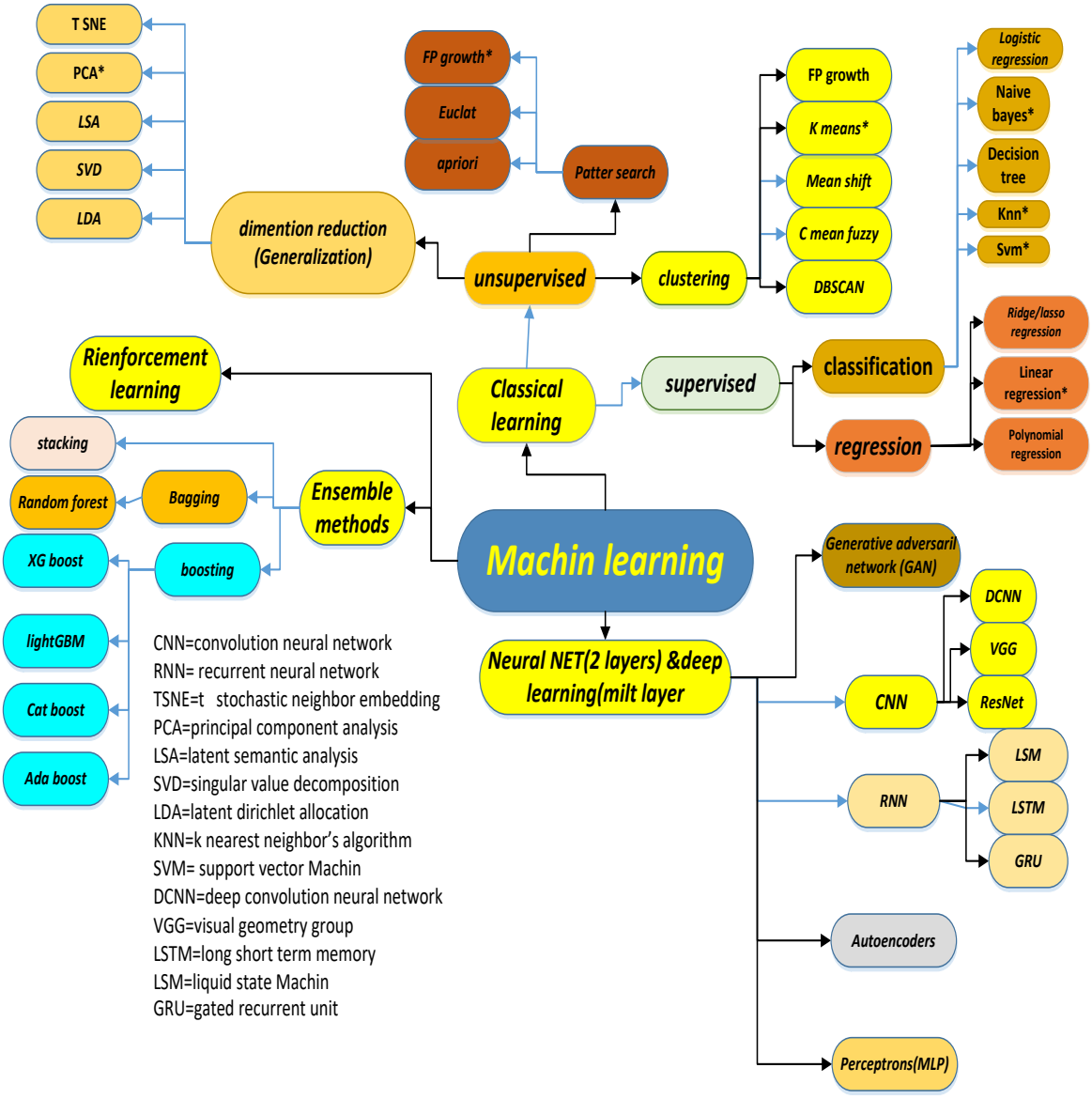

Figure 2.1. The main Machin learning methods [29].

2.2.2.Image Classification:

Classification of brain MRI is essential for differentiating between abnormal and normal tumor regions. With regard to the object or kind of image that each feature in an image represents, the aim of image classification is to pinpoint a specific gray level (or color) for each feature. The classification is carried out using multispectral data, and the categorization's numerical value is determined by whether each pixel's data contains a spectral pattern [27].

Data is categorized using image features' numerical properties in image classification. Classification algorithms are constructed in two stages: training and testing. During the beginning training stage, common image feature characteristics are separated and utilized to generate a distinct definition of every classification group, such as the training class. These feature-space partitions are then used to classify image features in the subsequent testing phase[28].

The description of training classes is a critical step in the classification process. In supervised classification, mathematical processes (based on prior understanding of likelihood distribution functions) or transfer processes can be used to extract class descriptive terms. In unsupervised classification, clustering algorithms are employed to instantly segment training phase into prototype classes[30].

Preprocessing, Feature Extraction, and Classification constitute the classification model's fundamental steps.

2.2.3.Preprocessing

The hardest and most crucial step in computer-aided segmentation is preprocessing. Each image must be preprocessed before any algorithm can be applied to it. Because the intensities of the same different tissues differ on

different scales. This noise reduces the precision with which irregularities are detected [31][32][33].

Another helpful tool for image preprocessing is filtering. Using a filtering technique, you can enhance or modify an image to draw attention to some details while hiding others. Image filtering includes techniques like edge enhancement, sharpening, and smoothing. Frequency domain and spatial domain are the two categories of filters used in convolution, which is the application of filters to an image.

Spatial domain filters for denoising and edge detection from MRI images include mean, median, Gaussian, Laplacian, gradient, and mid-point filters. Frequency domain image filtering, in contrast to spatial domain enhancement, is an image enhancement method that improves images specifically for a given application. To improve images, frequency domain filtering techniques include low pass, high pass, fast Fourier transformation, ideal, Butterworth, and Gaussian filters [16]. In order to achieve frequency-domain filtering, the Fourier transform of the target image is modified. The target image is then recovered from the frequency-domain filter by taking the inverse Fourier transform [34].

2.2.4. Feature Extraction

The amount of data required to accurately represent a brain MRI requires a significant amount of memory and processing time. To reduce the amount of time and information that must be stored in memory, features from an image are extracted [11]. Relevant data from the image is included in the features that were extracted. It can be used as a classifier input for categorizing and segmenting brain image data. The region of interest (ROI) for brain MRI images differs from normal and abnormal in the traits that set them apart. The intensity of the tumor is typically higher than the intensity

of the surrounding normal tissue. Other crucial texture characteristics include contrast, entropy, homogeneity, and others. It is crucial to understand how these characteristics are applied when attempting to differentiate the tumor from other normal tissues [35]. The right feature extraction is crucial for tumor detection from brain MRI images. According to the claim, three different types of parameters can be extracted while accounting for information loss and accurate feature extraction. The first three are made up of shape feature variables (such as area, irregularity, and circularity), the second is made up of intensity feature parameters (such as mean, variance, and standard deviation), and the third is made up of texture feature variables (contrast, correlation, entropy, etc.) [11]. Features based on intensity Analyze the likeness, homogeneity, brightness, and darkness of the images, as well as their heterogeneity, which is strongly associated with the variations in the brain MRI. The texture feature separates cerebrospinal fluid, tumor, gray matter, and white matter in MRI of the brain. An image's texture is distinctive because it offers a higher-order characterization of the image and details on the spatial distribution of tone color variations or gray tones. It is possible to specify the homogeneity or likeness between image regions using texture extraction . Excessive features increase computation times and memory requirements. The "curse of dimensionality" refers to the fact that they can occasionally make classification more difficult. Features must be trimmed down in number. The smallest number of dimensions in the best subset for feature selection results in high accuracy while excluding the additional, unimportant dimensions. We are getting ready for training and testing on key MRI feature extractions. The objective of the MRI image identification system is to compare MRI image samples used for training and testing [30]. It is evident from the discussion above that the process of extraction, reduction, and selection features is incredibly crucial for tumor detection and classification from brain MRI. Statistical feature extraction

techniques include texture-based techniques like the Gray Level Co-occurrence Matrix (GLCM), the Histogram Of Oriented Gradient (HOG), the Discrete Wavelet Transform (DWT), the Principal Component Analysis (PCA), and the Independent Component Analysis (ICA) [36].

Histogram of Oriented Gradients (HOG): The Histogram of Oriented Gradients was developed by Dalal and Triggs as a method for identifying object in pictures. The feature descriptor's objective is to generalize the object in an image so that it yields the same feature descriptors in images containing that object and was taken under various conditions, such as different angles, lighting, distance, and so on. The HOG descriptor technique counts gradient orientation occurrences in localized portions of an image-detection window, or region of interest [37][38].

The images are initially divided into cells by HOG. Cells can have a rectangular shape or a radial shape.

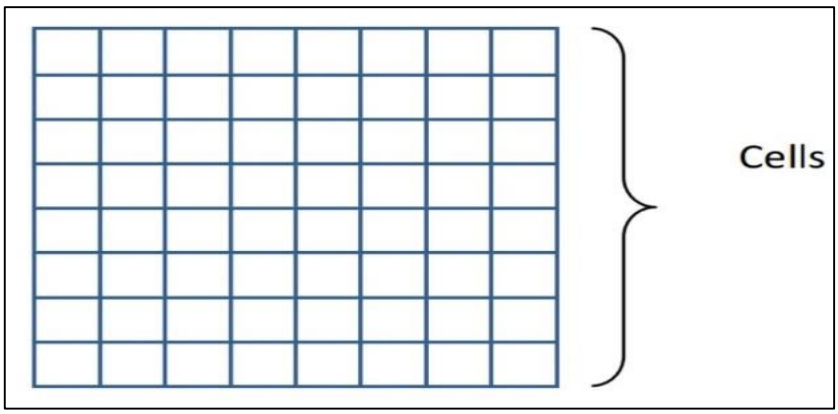

Figure 2.2. Dividing the image into cells[39].

The image has been split up into sections that are linked together, known as cells, in this method. The cells generate a histogram of oriented gradients. The image gradient in the x and y directions is represented by G_x, G_y. Equations (2.1) and (2.2) are used to compute the image gradient's magnitude and angle for each pixel.

$$|G_i(i,j)| = \sqrt{G_x(i,j)^2 + G_y(i,j)^2} \quad \text{..... (2.1)}$$

$$\theta_g(i,j) = \arctan\left(\frac{G_y(i,j)}{G_x(i,j)}\right) \quad \text{.....(2.2)}$$

Where $|G|$ represents the magnitude of the gradient, and θ_g represents the angle of the gradient, i represent the rows and j represent the columns of the image. In order to compute the HOG, the angle is divided into n equal distances, where n denoted the number of gradient directions or histogram bins. To compute the histogram, each pixel within the cell votes for one of the histogram bins based on its gradient angle, as demonstrated in figure (2.3). In this pixel, these votes are weighted according to the gradient size[37].

Following the calculation of the gradient histogram for every cell, the central pixel of the cell receives this histogram. As a result, an n-dimensional vector is created for each pixel, which represents the gradient histogram of its surroundings, is calculated. Equation (2.3) is used to normalize this vector.

$$v = \frac{v_i}{\sqrt{\sum_{i=1}^{n} {v_i}^2}} \quad \text{.....(2.3)}$$

38	84	69	102	124	40
48	93	80	50	140	67
56		94	84	90	141
106	55	144	53	83	91
96	105	87	132	52	90
35	82	123	92	57	48

$\begin{bmatrix} 38 \\ 38 \end{bmatrix}$

These are the gradients in *X* and *Y* directions (see eq.2.1 and 2.2)

Figure 2.3. Values of pixels in a cell's zoomed-out version[37]

2.3. Classification

Classification is the process of grouping similar classes of input patterns. Despite the wide variety of classification techniques available for brain tumor detection, the detection rate is still insufficient. Additionally, the success or failure of image classification depends on accurate image partitioning into meaningful regions [40]. Many factors must be considered when choosing a suitable classifier: Classification accuracy, Algorithm performance, and Computational resources.

Supervised methods classify unlabeled data from the testing phase using accurately labeled data from the training phase [41]. It consists of two stages: training and testing. Throughout this phase of training, a model is created that maps the extracted data features, refers to labels or classes that the model is then utilized to calculate during the testing phase, unlabeled data classes were created in terms of classification accuracy, supervised classification outperforms unsupervised classification during the training period, demonstrating the variability of results[42].

2.3.1. k-Nearest Neighbor

The (KNN) classification algorithm is one of the most fundamental in the supervised learning domain. It is depended on feature similarity, which is computed by comparing an unknown data point's similarity to the training dataset. It also determines how a given data point is classified. The following describes how the KNN algorithm is trained [43]:

1) Together with the new sample, a positive integer value k is defined.

2) Choose the k values in our database that are most similar to the new testing sample.

3) We determine which of these entries has the most similar classification.

4) Using the value of k, we assign a classification to the new sample.

5) If you don't get satisfactory results, try changing the value of k until you do.

2.3.2. Support Vector Machine (SVM):

The fundamental SVM is a non-probabilistic binary linear classifier that takes a set of input data and predicts which of two potential classes will make up each given output. SVMs can successfully operate linear classification in addition to non-linear classification by employing a kernel trick that essentially maps their inputs into high-dimensional feature spaces. In order to maximize the margin between classes, its kernel is used to minimize empirical risk and control class assignment [20]. SVM consists of two phases: training and testing. SVM learns by feeding input into its learning algorithm from features. During training, SVM picks the right margins between two classes. Features are categorized in accordance with their membership in a specific class. This method axiomatically reduces the complexity and computation required to solve the problem.

SVM has the following advantages: accuracy, high dimensionality because it operates efficiently in high dimensional spaces ($\geq 10^6$), efficiency because it only uses a subset of training points, effectiveness on smaller, clean datasets, and memory efficiency because only these points are stored in memory when making decisions because only subsets of training points are utilized in the decision-making process of assigning new members [44]. SVM is based on the idea of locating the best hyperplane for dividing a data set. This is illustrated in figure (2.4) [20].

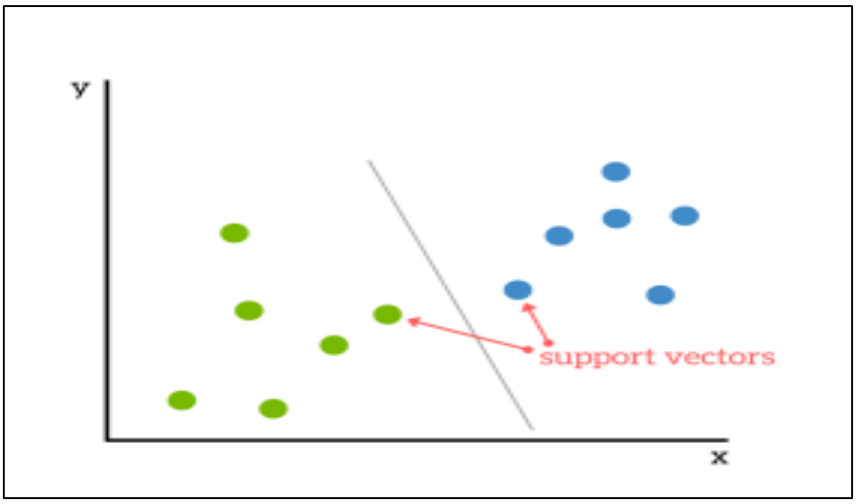

Figure 2.4. Hyperplane-based classification of the dataset [20].

2.3.3.Random Forests

With no variable elimination and the ability to process tens of thousands of input instances, random forest is an easy-to-use managed classification technology that excels at handling large datasets. It is comparatively resilient to noise and outliers. In contrast, the attribute of each tree is frequently selected at random, and each tree builds itself in a distinctive manner that differs from other trees in the same forest. Each decision tree in the forest will then determine what class (for classification) these decided to enter data belong to, and the method will choose the class with the highest level of specificity (Majority Voting) [12].

2.3.4.Artificial Neural Network:

The biological neuron: Information is processed by a unique type of biological cell called a neuron. Each neuron in the human brain is connected to between 10^3 and 10^4other neurons, according to which states that there are approximately 10^{11} neurons in total. The total number of connections is between 10^{14} and 10^{15}. A typical neuron is composed primarily of the following three components, as shown in figure (2.5):

− Neuron inputs called dendrites are responsible for gathering electrical data from the nervous system.

− The soma processes this data before returning an impulse-type electrical signal.

− The incoming signal is sent to nearby neurons via the axon.

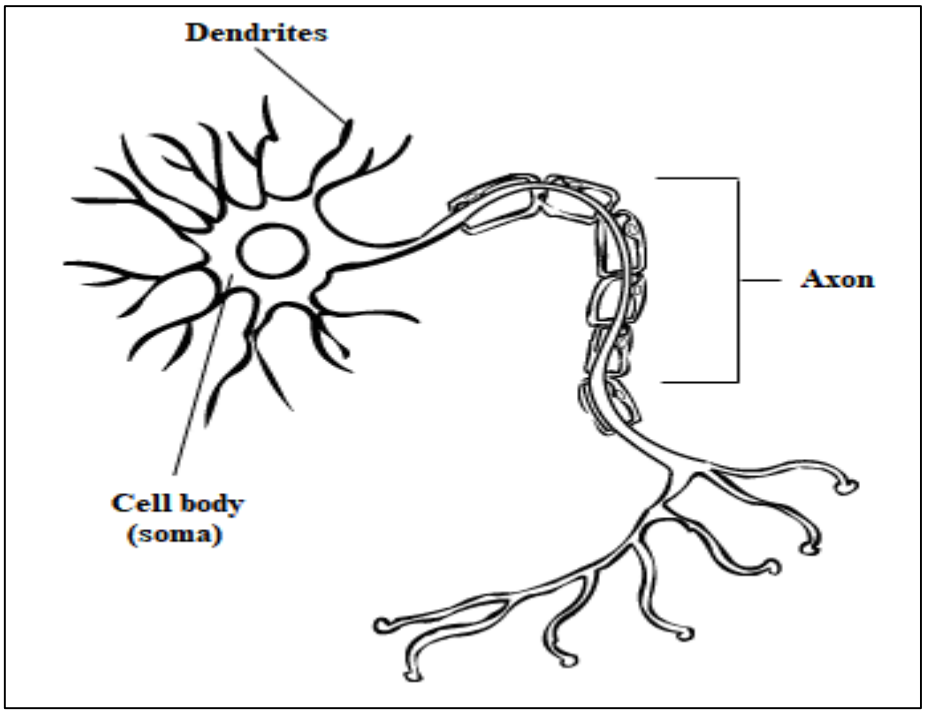

Figure 2.5. The biological neuron[45].

The formal neuron: A neural network (NN), also known as an artificial neural network (ANN), is a mathematical model or computational model inspired by the structure and/or functional aspects of biological neural networks. A neural network is made up an interconnected network of artificial neurons (processing elements) that work together to solve specific problems. ANNs, like humans, learn by example. The neuron operates in two modes: training/learning and using/testing[37]. In most cases, an ANN is an adaptive system that changes its structure in response to external or internal information that flows through the network during the learning phase. Neural networks are nonlinear statistical data modeling tools that have recently

emerged. They are typically used to model complex relationships between inputs and outputs or to search for patterns in data [46].

For pattern recognition and other related issues, ANNs are frequently used. Neurons and their weighted connections comprise ANNs. The arrangement of neurons forms layers, and weighted connections link the neurons in the various layers. According to the synaptic potency of neuron connections, each connection is given a weight. Both an ANN's weights and its input-output function, or transfer function, affect how the ANN behaves. Figures (2.6) illustrate how this function can be categorized as either linear, step, or sigmoid.

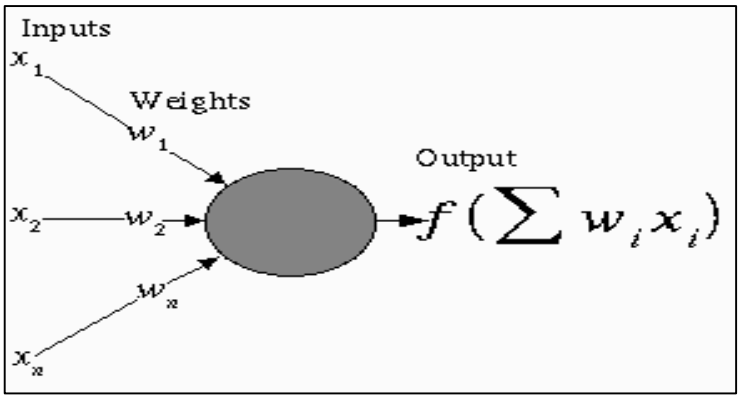

Figure 2.6. Structure and functioning of a single neuron [46].

A supervised learning algorithm is the Back Propagation learning algorithm. It is one of the most significant advances in neural networks as shown in figure (2.7). Back-Propagation Learning Networks are the networks associated with the back-propagation learning algorithm (BPNs) [38]. This algorithm provides a procedure for changing the weights in a BPN to correctly classify an input for a given set of training input-output pairs. This weight update algorithm is based on the gradient-descent method, which is commonly used in simple perceptron networks with differentiable units. The error is sent back to the hidden unit in this manner. The objective of the neural network is to train the network to find a balance between its

capacity for response (memorization) and its capacity for reasonable responses to input that is comparable but not exactly the same as one used in training (generalization).

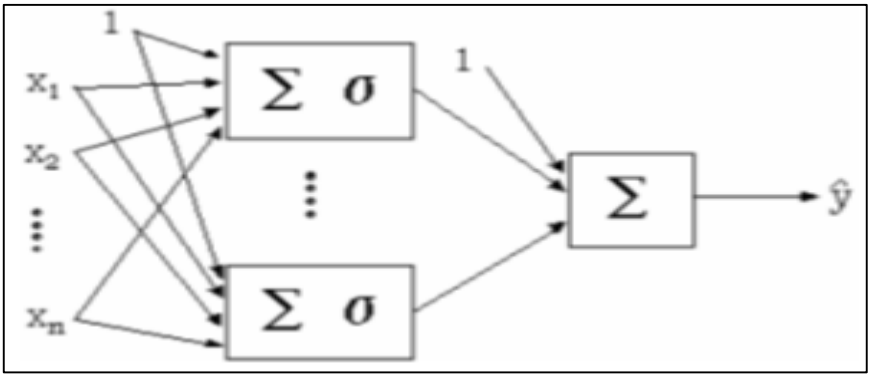

Figure 2.7. Neural network Feed forward architecture [45].

BPN algorithm stages include weight initialization, feedforward, backpropagation of error, and weight and bias updating.

2.4. Segmentation:

A process called segmentation divides an image into distinct regions according to factors such as contrast, brightness, brightness level, and texture. In medical images, segmentation serves the following purposes [34]

1. Calculating ROI.
2. To examine the anatomical makeup of various body parts.
3. Estimating the tumor's size.
4. The radiation therapist can use it to help the radiologist plan the dosage of radiation.

Brain segmentation methods are classified according to their underlying principles. For medical purposes, MRI segmentation methods are classified as follows[38]: Manual, Semi-automatic, Fully-automatic, and Hybrid segmentation.

i. Manual segmentation is the process of labeling and dividing boundaries in an image by a skilled and experienced human operator. With the help of this segmentation, anatomical structures will be hand-painted and labeled in the manner of slice-by-slice volumetric imagery [47]. The manual segmentation technique is said to be more precise. In order to detect lesions with different labels and segment brain tumors, this method is used to define the boundaries and structures of interest. In addition to being time-consuming and error-prone, manual segmentation also requires the operator to spend a lot of time analyzing the data using intra- or inter-variability studies. For basic formations in atlas-based segmentation techniques of various brain structures, the brain atlas for manual segmentation has been used [12]. In order to overcome the limitations of manual segmentation, semi-automatic and fully automatic segmentation techniques have been developed [44].

ii. Semiautomatic: This segmentation is semiautomatic, with the operator defining the area of interest. Using algorithms like (SIOX)simple interactive object extraction livewire, the image is processed to get the ideal edge fits. To receive a response from the computing software, the human expert in information perception analysis must first provide some input parameters. The main processes of semi-automatic segmentation are initialization, feedback response, and evaluation[40]. Results from fully automatic segmentation techniques outperform those from semi-automatic techniques.

iii. Fully automatic: The computer determines segmentation in the fully automatic segmentation method, which does not require any human operator assistance. Fully automatic segmentation methods use algorithms that combine artificial perception and prior knowledge [47].

iv. Hybrid segmentation: The hybrid segmentation technique combines any number of segmentation techniques to produce improved results in terms of accuracy and computational time.

By removing artifacts when non-sharp edges are present in an image using the appropriate filtering, tumor segmentation will perform better in terms of precision, duration, and the quantity of necessary iterations. Motion artifacts may be eliminated using a suitable restoration technique [30]. Nowadays, segmentation algorithms primarily rely on the gray level, and, texture-based techniques.

For the purpose of segmenting brain tumors from MRI images, the following methods have been put forth in this work: The most widely used methods for this are model-based, pixel classification, region-based, and threshold-based methods [40].

2.4.1. Thresholding Based Segmentation By comparing image objects intensities up to a few intensity thresholds, thresholding is a quick and efficient method for segmenting regions of an image. Both global and local thresholds are possible. When an image's histogram displays a bimodal pattern, global be used to isolate the object from the surrounding area. If the image has more than two different kinds of regions, each of which corresponds to a different object, the segmentation must be performed using local thresholding. The image can be segmented using multiple individual thresholds or a multi-thresholding technique. Applying this approach, the image is divided directly into different regions based on the intensity values [48]. There are two different kinds: 1) Global thresholds and 2) Local thresholds.

2.4.1.1. Global Thresholding:

Intensity is the most basic shared property between pixels in a region. Because of this, segmenting such regions by separating light from dark areas is called thresholding. By setting all pixels to zero below a specific threshold and to one above that threshold, thresholding transforms grayscale images

into binary images[8]. If $g\ (x, y)$ at some global threshold P is a thresholded version of $f\ (x, y)$,

$$g(i,j) = \begin{cases} 1 & if \quad f(x,y) \geq p \\ 0 & otherwise \end{cases} \ldots\ldots\ldots\ldots\ldots\ldots\ldots\ldots\ldots\ldots (2.4)$$

which assigns a value of 1 to pixels that are in the ROI and a value of 0 to pixels that are in the background.

Thresholding's primary drawback is that it ignores any relationships between the pixels and instead only considers the intensity of an image. Contiguous pixels may not always be detected by the thresholding procedure. Unwanted pixels are easily added as extras, and occasionally separated pixels inside the region (particularly near its borders) are disregarded [49]. Simply put, as the noise level increases, these effects worsen because it is more probable that a pixel's intensity won't match the average intensity in the area. It is important to experiment with thresholding, sometimes gaining too many background pixels and sometimes losing too much of the region. Additionally, Shadows cast by objects in the image can be problematic, especially when they accidentally become a part of a dark object against a light background or when they cross over with another object [31]. The fact that some areas of the image may appear brighter and others may appear darker without any correlation to the objects in the image is another issue with global thresholding [50].

Global works well when an image has homogeneous objects or when the background and objects have a high degree of contrast. On the other hand, if the intensity levels of two or more tissue structures overlap, It could fail and not produce fully automatic segmentation. The accuracy of the ROI is also in doubt because it separates itself from the background by using a single threshold value that might be extremely significant statistically. As

the quantity of regions, the level of noise, or the contrast of the image decreases, threshold selection becomes more difficult [8].

2.4.1.2. Local Thresholding

Numerous thresholding techniques are categorized as local thresholding in addition to global thresholding. Within a pixel's vicinity, a local threshold is determined adaptively. These techniques may be useful when a thresholding value for the entire image cannot be determined from a histogram or when a single threshold does not provide good segmentation results. By estimating a threshold value for each area of the intensity histogram, one can determine the local threshold. Partial volumes of each region can be calculated to estimate the local threshold values for MR image segmentation, as can local statistical properties like the mean intensity value in T1-weighted MRI [10] [51].

2.4.2. Pixel Classification:

Segmentation techniques can also be classified by pixels. In feature space, Pixel attributes are a way of describing the pixels in an image, which can include each pixel's local texture, gray level, and color. Image segmentation can be carried out in a one-dimensional feature space, and gray level is typically used to categorize pixels in a single-frame (or single-channel) image. Images with multiple frames or multiple modalities can be segmented using multidimensional feature space.

Methods that utilize pixel classification that is used to segment brain tumors are restricted to clustering pixels in the feature space using either supervised or unsupervised classifiers [52].

2.4.2.1. Unsupervised Methods:

Unsupervised segmentation can combine pixels with similar traits without the use of training data. Based on features of an image, like intensity,

texture, or gradient, an algorithm establishes the number of classes. These techniques can handle more complicated problems[53].

Unlabeled image data are divided into clusters using the unsupervised pixel-based segmentation technique known as clustering. These clusters are based on the shared traits of the pixels. In the feature space, the separation between two vectors, which has the form, offers a clear measure of similarity:

$$d(x_i, x_j) = \left(\sum_{k=1}^{n} \|x_i - x_j\|^p \right)^{\frac{1}{p}} \dots\dots\dots\dots\dots\dots\dots\dots\dots\dots\dots (2.5)$$

where the two vectors in the feature space $x_i = (x_i{}^1, \dots, x_i{}^n)$ R^n and $x_j = (x_j{}^1, \dots, x_j{}^n)$ R^n are concerned As can be seen, when $p = 2$ and 1, respectively, the aforementioned measurement corresponds to Euclidean distance and Mahalanobis distance.

The normalized inner product, which can be calculated as follows, is another indicator that is frequently used as a similarity criterion:

$$nd(x_i, x_j) = \frac{x_i{}^T x_j}{\|x_i\| \|x_j\|} \dots\dots\dots\dots\dots\dots\dots\dots\dots\dots\dots\dots\dots (2.6)$$

where T stands for the operation of transposing a vector. The cosine between the feature space vectors x_i and x_j is disclosed by this measurement. Usually, similarity within each cluster and dissimilarity between clusters are taken into account as part of the cost function that optimizes cluster formation. The centroid (or mean) and variability of each cluster, which denote how compact the objects within the cluster are, serve as a representation of the cluster. Hard clustering and soft clustering are the two types of clustering. An information point belongs to a cluster either directly or indirectly in hard clustering. In contrast to k-means clustering, where

clusters do not overlap, soft clustering assigns a probability of cluster membership to each data point, even if it is not entirely contained within a cluster. Clusters can and often do cross over. Several clusters can simultaneously have one data point as a member, just like in fuzzy C-means clustering [16].

A classification that is unsupervised has the qualities listed below:

i) A full knowledge of the area is not necessary.
ii) Since a lot of the specific decisions necessary for supervised classification are not necessary for unsupervised classification, the operator has fewer opportunities to err.
iii) Unsupervised classification allows for the recognition of distinct classes as distinct units.

As opposed to unsupervised classification, which uses samples whose identities are known to classify unknown samples. A supervised classification has the following characteristics:

i) Requires in-depth knowledge of the subject.
ii) The labels include input patterns.
iii) Capable of detecting serious errors in training data and determining whether they have been correctly classified.

k-Means Clustering:

A crucial method used in pixel-based methods is k-Means clustering. The following few steps involve segmentation using the k-means algorithm. At first, it is assumed that k means $(m_1^{(1)}, m_2^{(1)}, \dots, m_k^{(1)})$ correspond to the k clusters of the image. Following that, the distance between each observation x_i, $i = 1,2,\dots,n$, where x_i is a real feature vector with d dimensions, and each cluster's mean $(m_j^{(t)})$, $j = 1,2,\dots,k$ is calculated. An observation shows that the cluster in which x_1 belongs has a mean with x_1's shortest

distance. Each time, a new mean is determined after a cluster of observations has formed. Till the new means are no longer changing, the previous steps are repeated. In the end, the image is divided into k clusters. The distance between each observation (x_i, $i = 1,2,\dots,n$), where x_i is a d-dimensional real feature vector, and the means $m_j^{(t)}$, $j = 1,2,\dots,n$ for each cluster at the t^{th} iteration are then calculated. An observation shows that x_1 is a member of the cluster whose mean is closest to x_1. A new mean is computed for each iteration after a cluster of observations has formed. Up until the new means stop changing, the previous steps are repeated. Consequently, the image is ultimately divided into k clusters.

The k-Means algorithm, while straightforward and computationally effective, may not always yield the best result, even after many iterations. In certain situations, a distance function other than Euclidean distance may produce convergent outcomes. O(knt), where k is the number of clusters, n is the number of data points, and t is the number of iterations needed typically k_n and t_n gives the algorithm's time complexity.

The initial cluster centers decide what value of t to use. A few restrictions apply to the k-Means algorithm, including the need to initialize the number of clusters k, choose the initial means, and take noise into account.

The k-means clustering technique is one of the most widely used hard clustering techniques in segmentation. This method falls under the category of unsupervised cluster analysis algorithms. The K-means algorithm is simple and easy to use [54][9]. Formalized paraphrase After the K-Means Clustering results are obtained, the threshold method is applied to the image to convert it from grayscale to binary. The image still produces noise after the threshold results are obtained. Mathematical morphology is used to

remove noise from the image, resulting in segmentation results that include the corpus callosum. This algorithm groups observations into clusters given an 'n' number of observations. When compared to observations from different clusters, those from the same cluster are similar. We assume that k, the number of clusters, is constant [40]. The "centroid" is the head of each cluster. Cluster centroids are initially given arbitrary values. The sum of squares of the separation between the observation and the cluster centroid is reduced iteratively. After that, iterations of the centroid are performed until convergence is achieved[9].

2.4.2.2. Supervised (Classification)

Supervised methods classify unlabeled data from the testing phase using accurately labeled data from the training phase [38]. It consists of two stages: training and testing. Throughout this phase of training, a model is built that maps the extracted data features. refers to labels, or, classes that the model is then used to calculate during the testing phase, unlabeled data classes were created in terms of classification accuracy, supervised classification outperforms unsupervised classification during the training period, demonstrating the variability of results. As a result, only a few classifiers are covered in depth[55].

2.4.3.Model-Based Segmentation Techniques:

The best techniques for separating brain tumor boundaries from 2D MRI data were examined in earlier sections. The segmentation of volumetric (3D) image data is a difficult problem that has mostly been addressed using model-based segmentation techniques such as parametric deformable models, geometric deformable models, or level sets. A priori information about the object, such as its shape, location, and orientation, is taken into account when creating a connected and continuous model for a particular anatomic structure for model-based segmentation. Some models are based

on statistical knowledge that was gathered from a population of training datasets in the past. The model is restricted globally by the statistical parameterization, and it can only deform in the ways that the training sets imply.

The variability of the relevant anatomic shapes makes it challenging to extract structures from medical images and reconstruct a concise geometric representation of these structures. The goal is to take boundary elements from a single structure and combine them into a model of the structure that is both consistent and coherent. For deformable models, it is necessary to construct a propagating interface, which has a speed defined by local, global, and independent properties and which can be either, a closed curve in 2D, or, a closed surface in 3D. Using the interface's original position and the associated speed function, deformable models can monitor the growth of a propagating interface during segmentation. Geometric and parametric deformable models are the two types that currently exist.

2.5. The performance evaluation of the proposed method:

An MRI of the brain is in the database. We have extracted, analyzed, and classified a vast array of images from various patients using our computerized system. Sensitivity, specificity, and accuracy—which are derived from the confusion matrix—have been used to categorize the results.

A) Confusion Matrix: Since calculating accuracy alone may be deceptive, it is better to illustrate correct and wrong instances of data using a confusion matrix. Figure (2.8) displays the proposed method's performance assessment using the confusion matrix technique for classifying abnormalities and brain tumors. It is a summary used to measure the effectiveness of a classification model in machine learning.

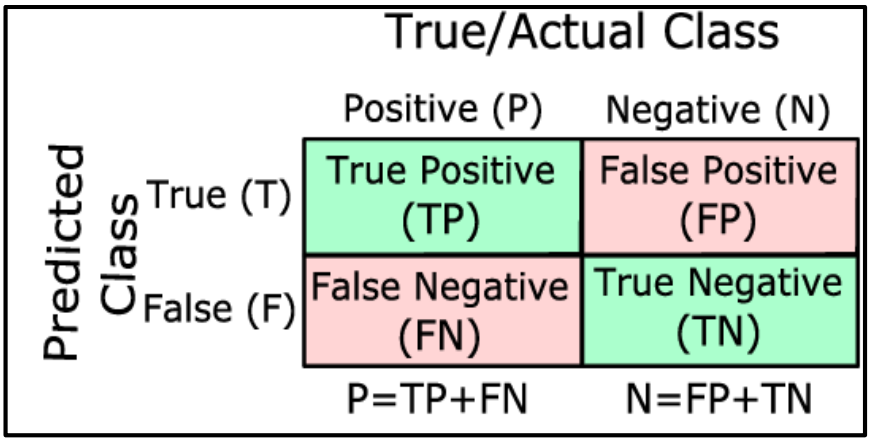

Figure 2.8 Confusion Matrix construction [42].

1. True Positive Rate (TPR):

It also goes by the name of sensitivity. It is described as a high percentage of correctly identified objects (Percentage of positive to detected points overall).

$$(\mathrm{TP}R) = \frac{TP}{(TP+FN)} \quad \text{.....(2.7)}$$

2. True Negative Rate (TNR):

It also goes by the name of specificity. A percentage of correctly identified items with negative proportions is how it is described [22] [23].

$$(\mathrm{TNR}) = \frac{TN}{(FP+TN)} \quad \text{.....(2.8)}$$

3. False-Positive Rate (FPR):

The term expectancy is another name for it. It is determined as a proportion between the number of negative events that were mistakenly labeled as positive (false positives) and the overall number of negative events (regardless of classification) [22] [23].

$$\mathrm{FP} = 1 - (\text{specificity}) \quad \text{.....(2.9)}$$

$$\text{False} - \text{positive rate: } \frac{FP}{N} = \frac{FP}{FP+TN} \quad \text{.....(2.10)}$$

4. False-Negative Rate (FNR):

This is a situation that actually occurred, despite claims to the contrary. That is incorrectly drawing a negative conclusion about the condition [22].

$$\text{FNR} = 1 - (\text{TPR}) \quad \text{.....(2.11)}$$

The accuracy, sensitivity, and specificity of the performance models used are compared across both training and testing samples.

B) Accuracy (ACC): To calculate the accuracy, divide the total number of correctly classified pixels by the total number of pixels in the image. It assesses an image's total proper pixels [48], which is computed as follows:

$$\text{Accuracy} = \frac{\text{TN+TP}}{(\text{TP+FP+TN+FN})} \quad \text{.....(2.12)}$$

C) Sensitivity (SE): The proportion of true positives correctly recognized is the sensitivity measure. It is used to recognize positive results based on test ability, in addition to the true positive rate, which is computed as follows [56]:

$$Sensitivity(SE) = \frac{TP}{TP+FN} \quad \text{.....(2.13)}$$

D) Specificity (Sp): The proportion of negative is an accurate measure of specificity. It is used to recognize negative results based on test ability, and the true negative rate is calculated as follows [56]:

$$Specificity(SP) = \frac{TN}{TN+FP} \quad \text{.....(2.14)}$$

E) K- Fold Stratified Cross-Validation:

One of the problems that occurs during the classifier training is overfitting, where the error on the training set is driven to a very small value, but when new data is presented to the network the error is large. Therefore,

cross validation is employed to avoid overfitting. In this thesis the K-fold cross validation is applied due to its properties as simple, easy, and using all data for training and validation. The mechanism is to create a K-fold partition of the whole dataset, repeat K times to use K-J folds for training and a left fold for validation, and finally average the error rates of K experiments. Figure (2.9) gives the basic structure of the “k-fold cross-validation method”.

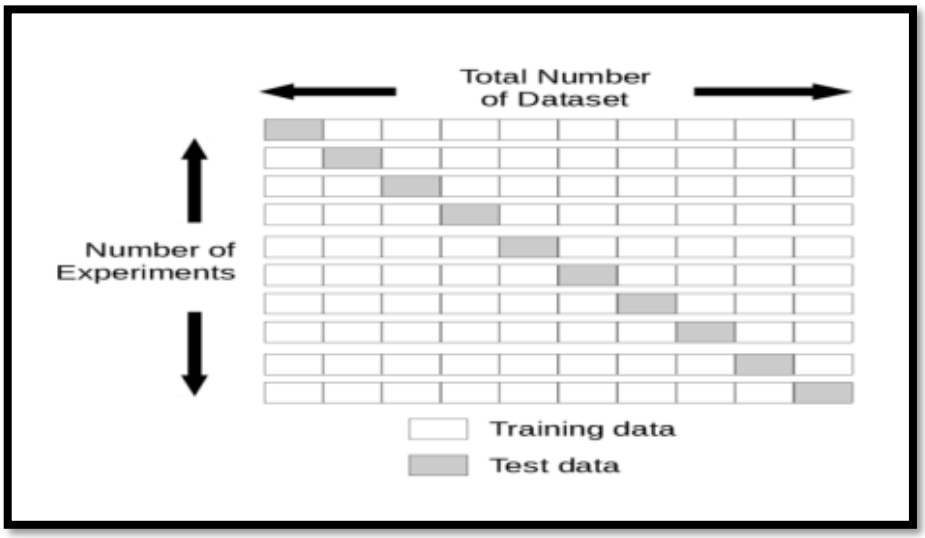

Figure 2.9. Basic k-folds for cross-validation [57].

Making a choice regarding the necessary number of folds is the difficult situation at hand. The "true error rate estimator" will have little bias if the K value is taken too high; however, the estimator's variance will be large and it will take more time to run. In contrast, if K is low, computation time will be reduced, the estimator's variance is low, but the estimator bias is higher [40]. Following this, the SVM is trained for each value while varying the "K values from 3 to 10" by a factor of 1. In order to obtain the "highest classification accuracy," we hereby select the best value of K.

The Jaccard distance has been utilized to compare the segmented picture to the ground truth image (manually segmented image by a radiologist). The Jaccard distance always has a magnitude between 0 and 1. The least

similarity was represented by a zero magnitude of Jaccard distance, whereas the greatest similarity was represented by one magnitude of Jaccard distance. The next formula was utilized to determine the Jaccard distance [30]:

$$JD = \frac{|A \cap B|}{|A \cup B|} \quad \text{.....(2.15)}$$

The segmented picture was B, while the ground truth image was A.

The coefficient of Dice represents the spatial relationship between these two binary pictures. This magnitude varies from 0 to 1 (uncorrelated areas versus those associated) (expected area). The formula is given [21]

$$DC = \frac{2\,|A \cap B|}{|A| + |B|} * 100 \quad \text{.....(2.16)}$$

The F-score, also called the F1-score, seems to be a metric for determining how accurate a model seems to be on a given dataset. The normal F1-score was calculated utilizing the average of recall and accuracy. The F1-score was determined in the following manner [31].

$$\text{F1 score} = \frac{2 * \text{precision} * \text{recall}}{\text{recall} + \text{precision}} \quad \text{.....(2.17)}$$

Chapter three

Methodology

Chapter Three

Methodology

3.1.Introduction:

The detection and segmentation of brain tumors using magnetic resonance imaging (MRI) is a critical step in medical image processing. This is due to the useful information obtained from MRI images, which aids the radiologist in brain diagnosis. Manual detection and segmentation of the tumor region from MRI slices is a sophisticated and time-consuming process, particularly when dealing with a large number of MRI images. As a result, an efficient and reliable detection model is proposed in this chapter which consists of two main steps: tumor slice detection and tumor region segmentation within the detected slice. During the detection step, features from each MRI slice are extracted using the Histogram of Oriented Gradient (HOG), and these slices are classified into the tumor and non-tumor images using three types of classifier models: (KNN), (SVM), or (ANN).

In the segmentation step, however, K-means clustering, thresholding, and morphological operations methods are used. By lowering the noise level, the median filter improves the quality of the MRI slices and the segmentation performance. Four morphological operations, erosion, dilation, closing, and opening, have shown significant improvements in the segmentation process. The experiments were run on two datasets, Kaggle and BRATS (high-grade (HGG) and low-grade (LGG) images, respectively). The results of the simulated experiments demonstrated the proposed algorithm's powerful achievements in terms of Dice, Jaccard, and F1 score. Furthermore, when applied to the same images, the proposed method outperforms a few other techniques. Figure (3.1) depicts the framework of the proposed brain tumor detection technique. It consists of detection and segmentation. Matlab was

used to implement and test this algorithm. The later stages of this chapter will go into greater detail about Matlab's role in this work.

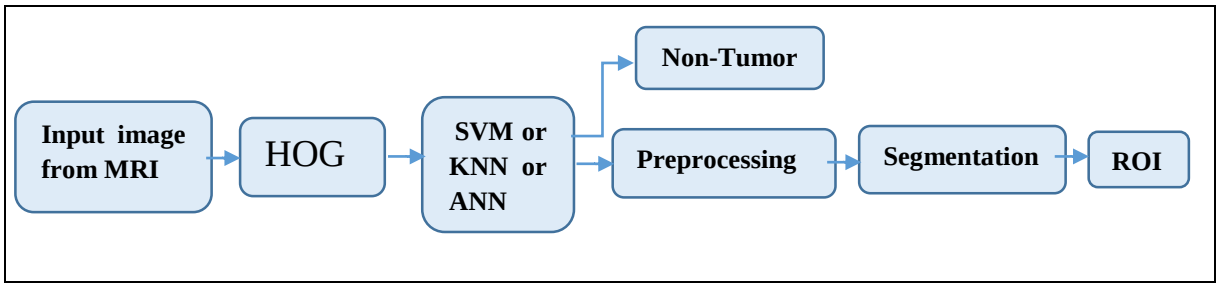

Figure 3.1. Block Diagram of the proposed system for tumor detection and segmentation.

3.2.Detection

In the detection of brain tumors. The database containing brain images must first be chosen. The next step is to use HOG to extract features from brain images. The following step is to label the extracted features and feed them into (SVM, KNN, and ANN). This will categorize the image as tumor or non-tumor. The final step is to evaluate the classifier performance using ROC characteristics such as accuracy, sensitivity, specificity, and confusion matrix.

3.2.1.Database:

Kaggle database was used in training of the detection image. This database contains 3000 brain MRI images. 1500 brain MRI Images with tumors and 1500 brain MRI Images without tumors[58]. Four samples of tumor images are demonstrated in figure (3.2)

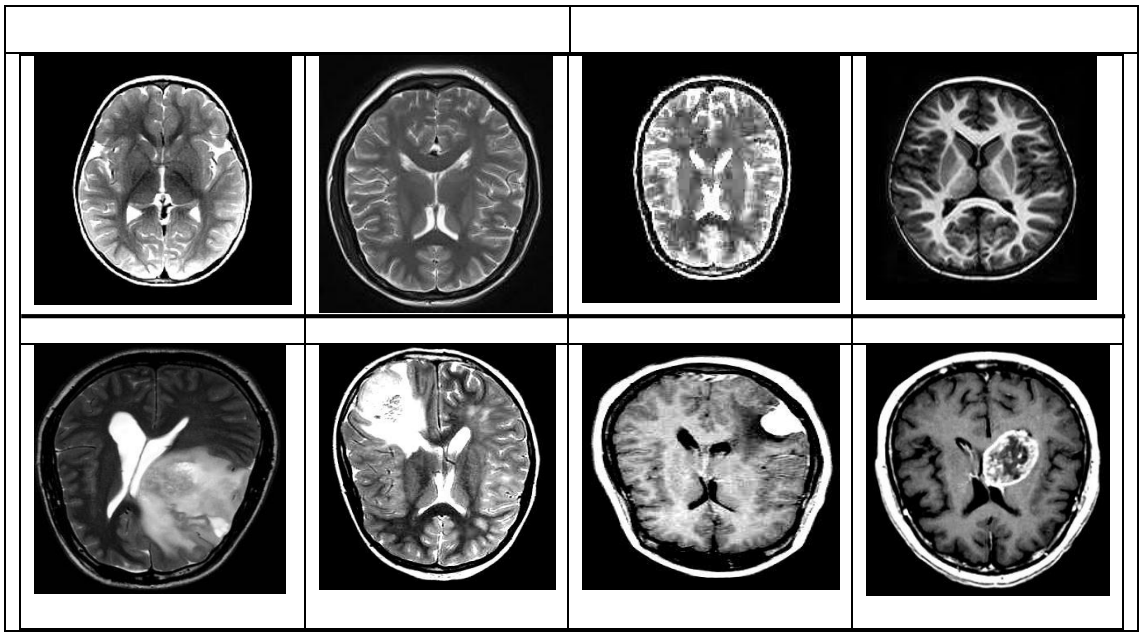

Figure 3.2. Sample images from the Kaggle dataset upper part brain MRI without tumor and the lower part brain MRI with tumor [58].

In the proposed method, the image size has been change into (128×128, 256×256, and 512×512).

3.2.2. Feature Extraction:

In this algorithm Histogram of Oriented Gradients (HOG) is used for feature extraction which is widely used in pattern recognition and computer vision. Particularly, they were used for pedestrian detection, and in combination with other spatial and temporal features that are used for multi-class object detection. Measuring the instances of gradient orientation in image-localized regions yields the HOG feature descriptor. In this thesis we attempt to detect tumorous regions in human brain MRI scan, using the HOG descriptors feature.

Histogram of Oriented Gradient (HOG):

The steps of HOG processing:

Step 1: The image is divided into small areas that are joined together, known as cells, in this method. A cell size of (8×8, 16×16, 32×32, and 64×64) is

taken as an optimum one because if we increase the cell size to [128 128] we might lose small-scale information.

Step 2: The different block sizes of the images are used to extract HOG features. 34696 features are produced by a block of size (512 512), 8100 features are produced by a block of size (256 256), and 1764 features are produced by a block of size (128 128).

Step 3 : Use MATLAB function to change cell size.

3.3. Classification:

For the purpose of separating brain tumors from non-tumor regions, brain MRI classification is essential. Image classification seeks to distinguish between a feature's color or gray level in relation to the thing or kind of image that feature represents. The classification is carried out using multispectral data, with each pixel's spectral pattern serving as the numerical foundation for classification. Using a numerical characteristics of image features, image classification categorizes data into groups. Two stages go into the development of classification algorithms: i) training and ii) testing. During the first training phase, common image feature characteristics are isolated and used to create a unique description for each training class or classification category. Following that, during the testing stage, these feature-space parts are used to classify image features.

The proposed method of supervised classification used (SVM), (KNN), and (ANN) based on classification accuracy (success classification rate).

3.3.1. Support Vector Machine:

The steps of SVM processing:

1) To detect an object in an image, the image's features must be fed into a recognition system, which in this case is SVM.

2) To feed SVM, the features of each image slice in subfolders of the training data folder was saved.

3) Made a m.file with labels for the images indicating 'tumor' or 'no tumor.'

4) The performance of SVM is evaluated using the ROC characteristics described in the following chapter.

5) The original values obtained from examining ground truth images are stored in 'labels' as '1' for 'tumor' and '0' for 'no tumor,' and SVM outputs are stored in 'scores,' which are also in binary format.

6) The range of K- Fold stratified cross-validation of SVM that used in this work is (1 to 10).

3.3.2.K-Nearest Neighbors (KNN):

The KNN classification algorithm is one of the most fundamental in the supervised learning domain. It is depended on feature similarity, which is computed by comparing an unknown data point's similarity to the training dataset. It also determines how a given data point is classified. The following describes how the KNN algorithm is trained:

1) The new sample and the positive integer value k are defined together..

2) Select the k values from database that most closely resemble the newly tested sample.

3) Determine which of these entries has the most similar classification.

4) Using the value of k, to assign a classification to the new sample.

5) If you don't get satisfactory results, try changing the value of k until you do.

Used k=5. The original values obtained from examining ground truth images are stored in 'labels' as '1' for 'tumor' and '0' for 'no tumor,' and KNN outputs are stored in 'scores,' which are also in binary format. And the range of K- Fold stratified cross-validation of KNN that used in this work is (1 to 10).

3.3.3.Artificial Neural Networks:

Back propagation network (BPNs) ANN approach is utilized in this work to classify the images as shown in figure (3.3).

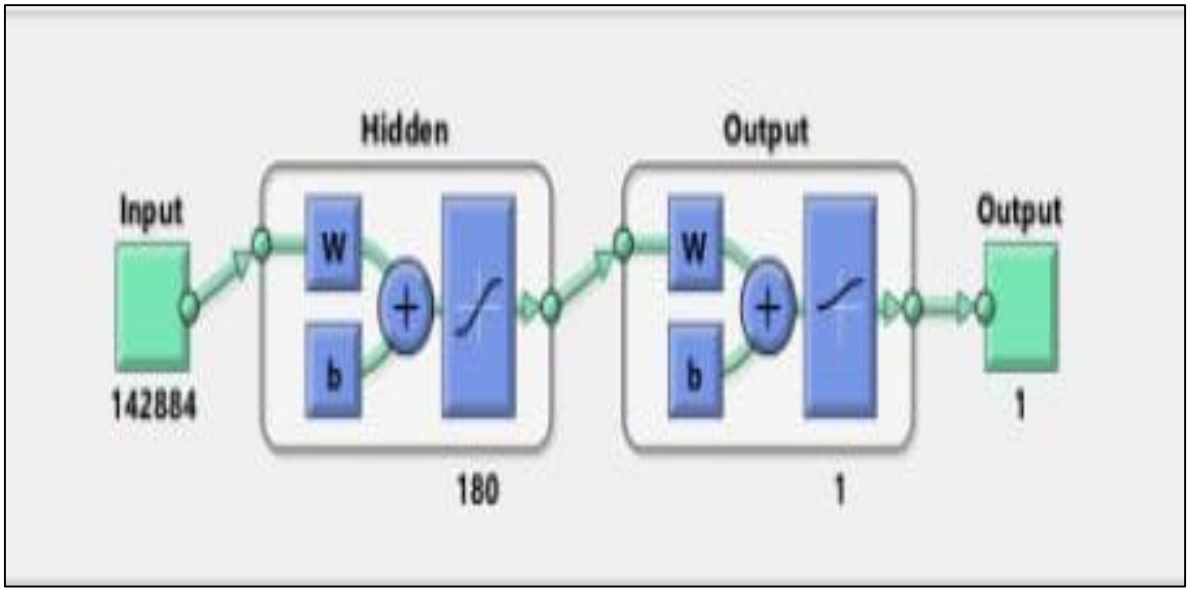

Figure 3.3. ANN Architecture

The samples are learned using a back propagation algorithm, the hidden and output layers are implemented using log sigmoid functions, respectively, and the weights are adjusted using Levenberg-Marquardt optimization (trainlm). A structure element known as a "block" is defined as each pixel and its surrounding small square neighborhood. A single image's

altered features are first extracted block by block to start the training process. Only the chosen features are extracted from a new image when we use it for classification, and the trained classifier is then used to determine whether the brain image contains a tumor or not. The number of input layer neurons n is fixed by the points number (features) is 142886, hidden Layer Size is 180 used by try and error in the output layer, we employ a single neuron. As depicted in figure (3.3).

The data were divided into training and testing --- the division ratios were done in three different ratios until determined the most accurate possible ratio of efficiency. The ratios that used are (70% Training, 15%Validation, and 15% Testing), (50% Training, 25%Validation, and 25% Testing) and (80% Training, 10%Validation, and 10% Testing).

3.4. Image Segmentation:

The location of the tumor on the given medical image must be identified in order to characterize the tumor. To delineate the ROI in the given image, the segmentation step subdivides the image into different regions based on certain properties. In this thesis, a proposed algorithm for segmenting brain tumors is proposed. The proposed algorithm is a hybrid model that combines unsupervised techniques like K-means Clustering with threshold-based segmentation. This algorithm employs morphological operations to remove no tumor regions from the resulting binary image. Because clustering is unsupervised, the proposed algorithm is efficient and less prone to errors. The methods used to create this algorithm are described in the following section. In Figure 3.4, the proposed algorithm 's framework for finding brain tumors is depicted. This algorithm was implemented and tested in Matlab.

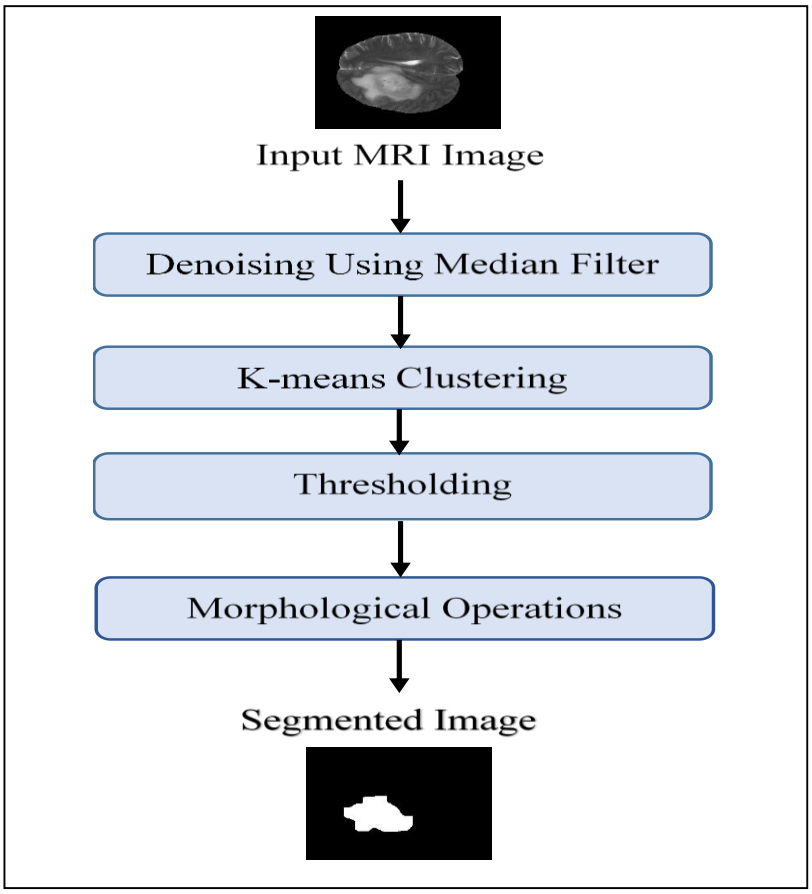

Figure 3.4. Block diagram of the suggested system for tumor segmentation

3.4.1.Database:

The brain tumor images employed in this algorithm were obtained from the Multimodal Brains Tumors Segmentation Challenge (BRATS). This dataset comprises 220 brain images with Highly-grade Gliomas (HGG) and 54 brain images with Low-Grade Gliomas (LGG). Four samples of tumor images are demonstrated in figure (3.5), along with its related ground truth region of interest images (ROI).

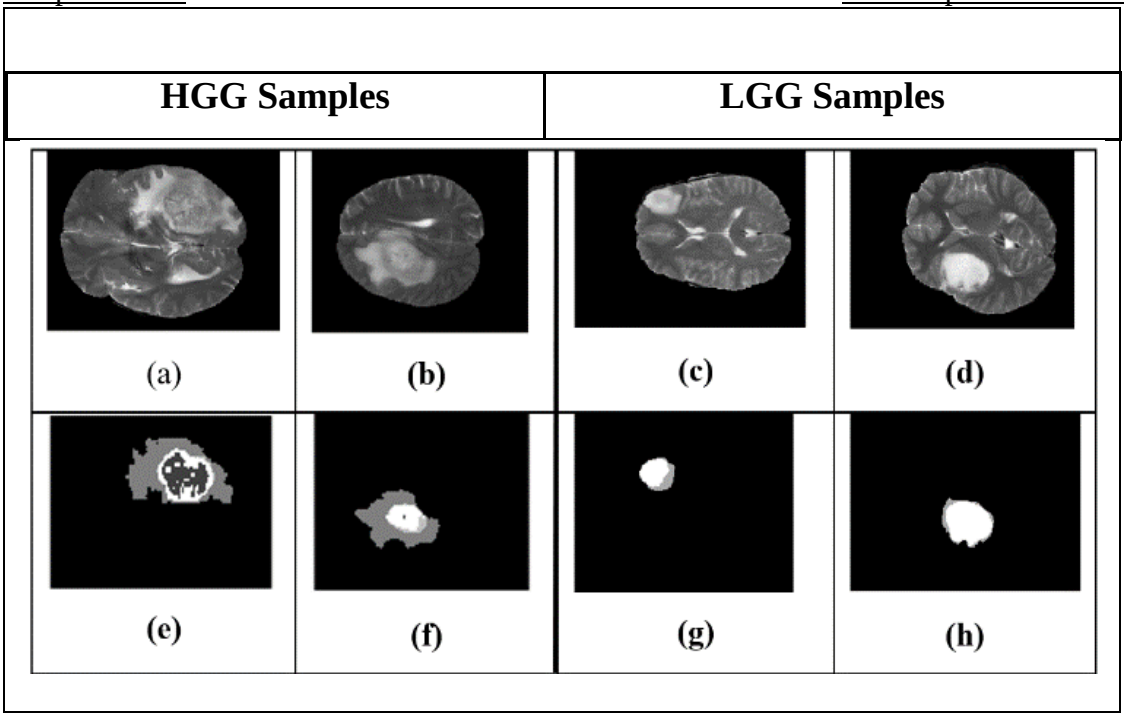

Figure 3.5. Sample images from the BRATS dataset and its manual expert segmentation (ground truth), upper part original images, and lower part ROI images.

3.4.2.Pre-Processing Using Median Filter:

As a preprocessing step, a median filter is applied to the image to improve the image quality and signal-to-noise ratio. This filter is built with a variable-size square window. The median filter method converts the central pixel magnitude in the scan window to the median magnitude of all pixels inside the window after sorting their magnitudes. The median filter approach has the advantage of rejecting certain types of noise very well, particularly impulsive noise with extreme magnitudes in some individual pixels. Edges are preserved while noise is removed; if necessary, the process can be repeated. This filtering algorithm improves the quality of MRI brain images. In our work, we applied a median filter with a window size of 5.

3.4.3. K-means clustering:

A difficult part of this method clustering is choosing the K-value. The initial K-value that was assigned has a direct impact on how well the segmentation process performs as a whole. Poor segmentation results are caused by the incorrect value, but this can be fixed by researchers by creating a new algorithm called adaptive K-means clustering. The initial value has no bearing on how quickly a cluster grows in this process. The K value is first chosen from the data set in the process. The seed point for clusters is generated by this K value. The characteristics of the element included in that particular cluster determine the cluster's characteristics.

In our work the K-Means clustering initially k centroid points are defined with k = 3.

3.4.4.Thresholding:

Thresholding is the process of transforming a grayscale image into a binary format depending on a threshold magnitude. It is one of the most basic segmentation techniques. The selection of a threshold magnitude is the main concern in this process. All gray level pixels below the threshold magnitude are set to zero (black), while those above the threshold magnitude are set to one (white) to create the binary image as shown in figure (3.12). A global threshold is utilized when a single threshold magnitude is specified for the entire image. For thresholding an image, this is the most intuitive method. It is simple and quick to compute that does not include any pixel-to-pixel relationships. In addition, it is suitable for the segmentation of images with no set shape because it does not require any prior shape knowledge.

3.4.5.Morphological Operation:

Mathematical morphology is a technique for extracting image components that can depict and describe region shapes like borders, skeletons, and the convex hull. Sets are utilized to define morphological

procedures. In image processing, morphology is utilized with two types of collections of pixels: objects and structuring elements (SEs) there is many type of structure element like (square, disc, and rectangular).

creates a square structuring element whose width is w pixels. Erosion, dilation, opening, and closing are the four morphological processes utilized in this technique. These operations are defined in set notation and use a structural element.

1. The Erosion:

The object is shrunk during the erosion process, resulting in a smaller size. The following is an erosion of the image A's (set's) erosion by component of structure B:

$$(A \oplus B) = \{(z|(\widehat{B})_z) \cap (A) \neq (\emptyset)\} \;\ldots\ldots\ldots\ldots\ldots\ldots\ldots\ldots\ldots\ldots\ldots.. (3,10)$$

The erosion process increases the number of pixels with zero (background) magnitude while lowering those with a magnitude of one (foreground). Furthermore, structures that are smaller than the structuring element are removed. As a result, it can eliminate the distracting relationship between two objects.

2. The Dilation:

The dilation process expands the size of an object. The following is the definition of the dilation of an image A by component of structure B:

$$(A\Theta B) = \{(z|(B)_z) \subseteq (A)\} \ldots\ldots\ldots\ldots\ldots\ldots\ldots\ldots\ldots\ldots\ldots\ldots\ldots (3,12)$$

Dilation raises the number of pixels with a magnitude of one (foreground) and lowers the number of pixels with a magnitude of zero (background).

3. The Opening:

An image opening results from a mix of degradation and dilatation. As following:

$$(AoB) = ((A \ominus B)) \oplus (A) \quad (3.14)$$

When structuring element B is "rolled" inside of boundary A, it reaches the boundary's extreme points, forming the boundary of the opened image. The opening procedure consists of a structuring element eroding an image, and the same structuring element dilates the resultant. In literature, the union set operation is also utilized to find the points of an opening image.

4. Closing:

A mixture of erosion and dilation processes is utilized to close a picture. It differs from the opening procedure regarding the order in which erosion and dilation occur. As following:

$$(A.B) = ((A \oplus B)) \ominus (B) \quad (3.16)$$

Given an image A and a structuring element B, the closure operation is performed by dilatation of image followed by erosion. Though the closure process softened features areas, it combines narrow breaks and thin gaps in general. As a result, it fills gaps in the object's edges and eliminates microscopic holes.

Chapter Four

Results and Discussion

Chapter Four

Results and Discussion

4.1.Introduction:

This chapter presents and discusses the experiments and their results that are applied using the proposed method explained in chapter three and their performance evaluation. The discussions of these experiments are divided into two parts, the first one is related to the detection of brain tumors and the second part is dedicated to brain tumor segmentation. All that is performed on a personal computer with an Intel Core i7 processor running at 2.20 GHz and 16.0 GB of RAM in the MATLAB 2019b environment.

4.2. Brain Tumor Detection Part:

The proposed method works on a brain tumor detection system based on machine learning algorithms. The primary goal of machine learning is to automate human assistance by training an algorithm on relevant data. The proposed work is divided into two parts: the first step is feature extraction using HOG and the second step is classification using (KNN, SVM, and ANN).

4.2.1 Experimental setup:

This section, explain the experimental setup of all methods that are used in brain tumor detection

A) Feature Extraction using HOG:

The image is divided into small areas that are joined together, known as cells, in this method. A cell size of (8×8, 16×16, 32×32, and 64×64) is taken as an optimum one because if we increase the cell size to [128 128]

we might lose small-scale information. The different block sizes of the images are used to extract HOG features. 34696 features are produced by a block of size (512 512), 8100 features are produced by a block of size (256 256), and 1764 features are produced by a block of size (128 128).

A large number of features must be extracted, which is both unnecessary and difficult, while a small number of features suggests a loss of sufficient information and have found that the image sizes of (256×256)produces better performance and it produces 8100 features with a cell size of (16×16).nFigure 4.1. shows non-tumor brain and tumor brain MRI and its HOG.

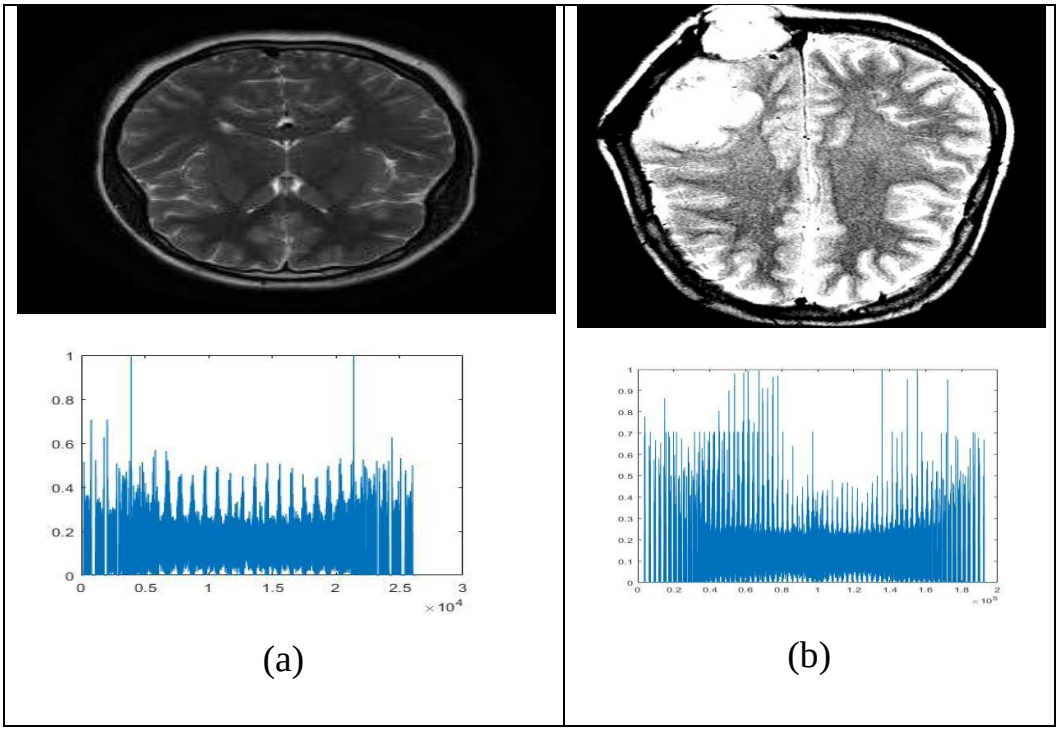

Figure 4.1. (a)Input non-tumor brain MRI and its HOG (b)Brain tumor MRI and its HOG

B) Classification:

In this algorithm three different classification models are used SVM, KNN, and ANN for the study of selected features. This helps to choose an appropriate classification strategy.

1) Support Vector Machines

In the Support Vector Machine, the K-fold has been changed to (3,5, 7, and 10) with each image size. the best results are achieved when K-fold is 10 and the image size is (256×256).

2) K-Nearest Neighbors

The K-fold has been changed into (3,5, 7, and 10) with each image size. the best results are appearing when K-fold is 10 and the templet of KNN is 3 the image size is (256×256).

3) Artificial neural network

In an artificial neural network (ANN), the hidden layer size is 180, and the ratios that we used are (70% Training, 15%Validation, and 15% Testing), (50% Training, 25%Validation, and 25% Testing) and (80% Training, 10%Validation, and 10% Testing).

4.2.2. The Simulation Results of Detection

This section will cover the results of applying the proposed method to the detection of brain tumor images and determined the most accurate possible ratio of efficiency, Sensitivity, and Specificity which are derived from the confusion matrix.

A)The SVM results

Changing the cell size of HOG into (16×16, 32×32, and 64×64) and the K.fold is (3, 5, 7, 10) apply this experimental setup to three image sizes:

1) when a block of image size (512×512) produces 34696 features, the higher accuracy was with (K.fold of SVM is 7, the cell size of HOG is(32×32))as illustrated in table (4.1), the higher sensitivity was with (K.fold of SVM is 10, the cell size of HOG is(16×16)) as illustrated in table

(4.2) and the higher Specificity was with (K.fold of SVM is 7, the cell size of HOG is(32×32)) as illustrated in table (4.3).

Table 4.1. SVM accuracy with image size (512×512)

K.Fold of SVM	The cell size of HOG		
	16×16	32×32	64×64
3	97.8	98.1	97.4
5	98.1	98.3	98.0
7	98.3	98.6	98.1
10	98.4	98.5	98.1

Table 4.2. SVM Sensitivity with image size (512×512)

K.Fold of SVM	The cell size of HOG		
	16×16	32×32	64×64
3	97.80	98.00	97.02
5	98.32	98.33	97.89
7	98.27	98.54	97.69
10	98.60	98.47	98.13

Table 4.3.SVM Specificity with image size (512×512)

K.Fold of SVM	The cell size of HOG		
	16×16	32×32	64×64
3	97.80	98.13	97.72
5	97.81	98.27	98.06
7	98.27	98.73	98.52
10	98.27	98.60	98.20

2) When a block of image size (256×256) produces 8100 features, the higher accuracy was with (K.fold of SVM is 10, the cell size of HOG is(16×16)) as illustrated in table (4.4), the higher sensitivity was with (K.fold of SVM is 10, the cell size of HOG is(16×16)) as illustrated in table (4.5) and the higher Specificity was with (K.fold of SVM is 7, the cell size of HOG is(16×16)) as illustrated in table (4.6).

Table 4.4. SVM accuracy with image size (256×256)

K.Fold Of SVM	The cell size of HOG		
	16×16	32×32	64×64
3	97.9	97.4	95.2
5	98.5	98.2	96.2
7	98.6	98.5	96.8
10	98.7	98.5	96.8

Table 4.5. SVM Sensitivity with image size (256×256)

K.Fold Of SVM	The cell size of HOG		
	16×16	32×32	64×64
3	98.00	97.27	93.91
5	98.79	98.46	95.41
7	98.73	98.40	96.25
10	98.93	98.53	96.13

Table 4.6. SVM Specificity with image size (256×256)

K.Fold Of SVM	The cell size of HOG		
	16×16	32×32	64×64
3	97.87	97.46	96.50
5	98.15	97.88	97.01
7	98.54	98.53	97.37
10	98.41	98.47	97.63

3) A block size of image size is (128×128) produces 1764 features, the higher accuracy was with (K.fold of SVM is 10, the cell size of HOG is(16×16)) as illustrated in table (4.7), the higher sensitivity was with (K.fold of SVM is 10, the cell size of HOG is(16×16)) as illustrated in table (4.8) and the higher Specificity was with (K.fold of SVM is 10, the cell size of HOG is(16×16)) as illustrated in table (4.9).

Table 4.7.SVM accuracy with image size (128×128)

K.Fold Of SVM	The cell size of HOG		
	16×16	32×32	64×64
3	97.5	96.1	83.3
5	98.0	97.1	84.2
7	98.3	97.4	84.2
10	98.4	97.4	84.7

Table 4.8. SVM Sensitivity with image size (128×128)

K.Fold Of SVM	The cell size of HOG		
	16×16	32×32	64×64
3	97.28	95.59	84.28
5	98.32	96.95	85.08
7	98.46	97.27	84.84
10	98.49	97.34	85.48

Table 4.9. SVM Specificity with image size (128×128)

K.Fold Of SVM	The cell size of HOG		
	16×16	32×32	64×64
3	97.79	96.69	82.37
5	97.75	97.32	83.30
7	98.14	97.46	83.52
10	98.40	97.46	83.95

From the results above we notice that the highest efficiency when the cell size of HOG is [16×16] with K.fold of SVM is 10 and image size is 256×256. When looking at figure (4.2), which represents the confusion matrix of the highest accuracy, the overall accuracy was 98.7%. Where the number of samples is 3000 images and the total features are 8100.

As seen in figure 4.2, a Matlab tool is used to create an SVM confusion matrix. A total of 1476 of the 1492 non-tumor MR images are correctly identified as belonging to the non-tumor target group, while the remaining 16 non-tumor images are misclassified as belonging to the tumor class target group. In 1508 tumor MR images, 1484 of the target classes are

correctly identified as being tumor, whereas 24 of the target classes are misidentified.

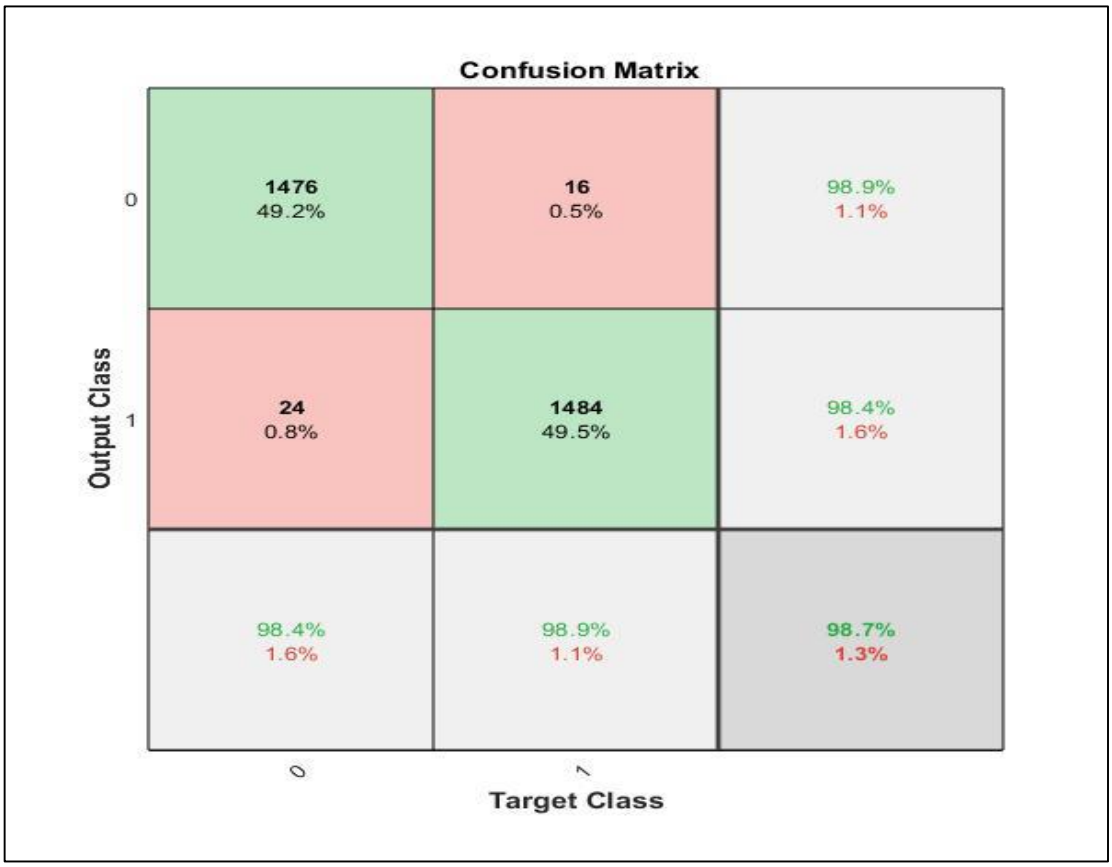

Figure 4.2. Confusion matrix (SVM model)

B) The KNN results:

Changing the cell size of HOG into (16×16, 32×32, and 64×64) pixels and the K.fold is (3, 5, 7, 10) we apply this experimental setup to three image sizes:

1) when a block of image size (512×512) produces 34696 features, the higher accuracy was with (K.fold of KNN is 10, the cell size of HOG is(16×16)) as illustrated in table (4.10), the higher sensitivity was with (K.fold of KNN is 10, the cell size of HOG is(16×16)) as illustrated in table (4.11) and the higher Specificity was with (K.fold of KNN is 10, the cell size of HOG is(64×64)) as illustrated in table (4.12).

Table 4.10. KNN accuracy with image size (512×512)

K.Fold Of KNN	The cell size of HOG		
	16×16	32×32	64×64
3	96.5	96.4	96.2
5	97.0	97.3	97.0
7	97.0	97.3	97.0
10	97.31	97.3	97.1

Table 4.11. KNN sensitivity with image size (512×512)

K.Fold Of KNN	The cell size of HOG		
	16×16	32×32	64×64
3	96.40	96.09	95.18
5	96.87	97.02	96.26
7	97.06	97.14	96.38
10	97.27	97.08	96.45

Table 4.12. KNN specificity with image size (512×512)

K.Fold Of KNN	The cell size of HOG		
	16×16	32×32	64×64
3	96.53	96.71	97.34
5	97.06	97.65	97.53
7	96.94	97.52	97.70
10	97.27	97.59	97.83

2) when a block of image size (256×256) produces 8100 features, the higher accuracy was with (K.fold of KNN is 10, the cell size of HOG is(16×16))as illustrated in table (4.13), the higher sensitivity was with (K.fold of KNN is 7, the cell size of HOG is(16×16)) as illustrated in table (4.14) and the higher Specificity was with (K.fold of KNN is 5, the cell size of HOG is (32×32)) as illustrated in table (4.15).

Table 4.13. KNN accuracy with image size (256×256)

K.Fold Of KNN	The cell size of HOG		
	16×16	32×32	64×64
3	96.2	96.3	95.5
5	97.4	97.2	96.0
7	97.4	97.3	96.4
10	97.5	97.3	96.4

Table 4.14. KNN sensitivity with image size (256×256)

K.Fold Of KNN	The cell size of HOG		
	16×16	32×32	64×64
3	95.78	95.30	93.66
5	96.96	96.46	94.46
7	97.28	96.83	95.20
10	97.21	96.64	95.02

Table 4.15. KNN specificity with image size (256×256)

K.Fold Of KNN	The cell size of HOG		
	16×16	32×32	64×64
3	96.70	97.34	97.43
5	97.78	97.97	97.72
7	97.59	97.78	97.74
10	97.72	97.91	97.80

3) when a block of image size (128×128) produces 1764 features, the higher accuracy was with (K.fold of KNN is 10, the cell size of HOG is(16×16)) as illustrated in table (4.16), the higher sensitivity was with (K.fold of KNN is 10, the cell size of HOG is (16×16)) as illustrated in table (4.17) and the higher Specificity was with (K.fold of KNN is 5, the cell size of HOG is (16×16)) as illustrated in table (4.18).

Table 4.16. KNN accuracy with image size (128 ×128)

K.Fold Of KNN	The cell size of HOG		
	16×16	32×32	64×64
3	93.3	95.4	91.3
5	96.9	96.3	92.9
7	96.9	96.3	93.4
10	97.1	96.3	93.9

Table 4.17. KNN sensitivity with image size (128×128)

K.Fold Of KNN	The cell size of HOG		
	16×16	32×32	64×64
3	93.20	93.32	89.74
5	95.53	94.83	91.87
7	95.77	94.90	92.66
10	96.03	94.95	93.35

Table 4.18. KNN specificity with image size (128×128)

K.Fold Of KNN	The cell size of HOG		
	16×16	32×32	64×64
3	97.69	97.62	93.06
5	98.28	97.80	93.98
7	98.07	97.87	94.10
10	98.23	97.80	94.46

From the results above we notice that the highest efficiency when the cell size of HOG is [16×16] with K.fold of KNN is 10 and image size is [256×256]. When looking at figure (4.3), which represents the confusion matrix of the highest accuracy, the overall accuracy was 97.5%. Where the number of samples is 3000 images and the total features is 8100.

In KNN confusion matrix, a total of 1466 of the 1508 non-tumor MR images are correctly identified as belonging to the non-tumor target group, while the remaining 42 non-tumor images are misclassified as belonging to the tumor class target group. In 1492 tumor MR images, 1458 of the

target classes are correctly identified as being tumor, whereas 34 of the target classes are misidentified.

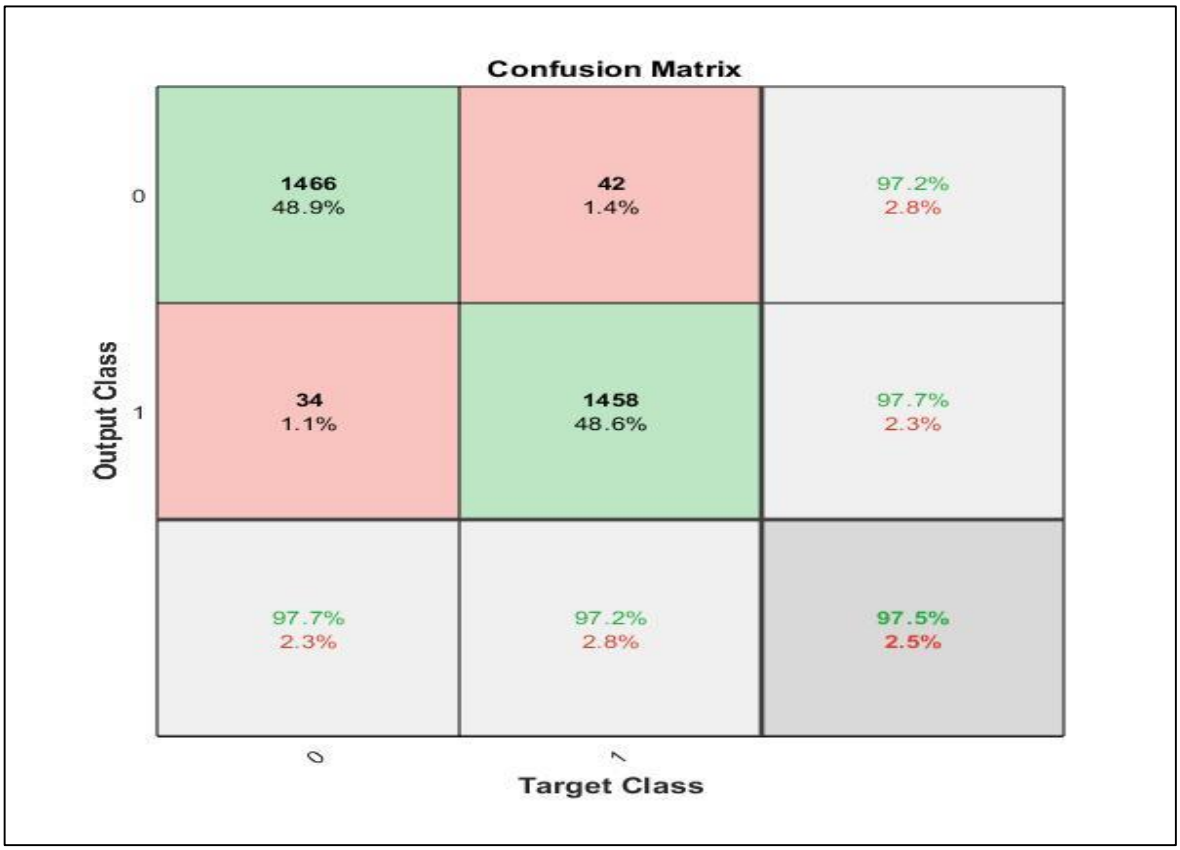

Figure 4.3. Confusion matrix (KNN model)

C) The ANN Results:

In the ANN model, the data was classified into two categories: training and testing. The division ratios were done in three different ratios until we determined the most accurate possible ratio of accuracy, sensitivity, and specificity by Resize the cell of HOG to (8×8, 16 ×16, and 32×32 pixels), the ratios that we used are (70% Training, 15%Validation, and 15% Testing), (50% Training, 25%Validation, and 25% Testing) and (80% Training, 10%Validation, and 10% Testing).

1) When the percentage of ANN (70% Training, 15%Validation, and 15% Testing) as illustrated in following tables [(4.19), (4.20), and (4.21)].

Table (4.19). ANN accuracy results in percentage (70, 15, 15).

Cell size Of HOG	Image size		
	512×512	256×256	128×128
8 × 8	99.3	99.0	99.4
16 × 16	94.9	99.3	99.0
32 × 32	99.5	98.3	99.2

Table (4.20). ANN sensitivity results in percentage (70, 15, 15).

Cell size Of HOG	Image size		
	512×512	256×256	128×128
8 × 8	97.84	96.82	98.08
16 × 16	95.00	97.60	98.34
32 × 32	98.56	97.10	97.93

Table (4.21). ANN specificity results in percentage (70, 15, 15).

Cell size Of HOG	Image size		
	512×512	256×256	128×128
8 × 8	98.17	96.09	97.11
16 × 16	94.78	97.11	96.65
32 × 32	96.70	93.30	97.13

2) When the percentage of ANN (50% Training, 25%Validation, and 25% Testing) as illustrated in following tables [(4.22), (4.23), and (4.24)].

Table (4.22). ANN accuracy results in percentage (50, 25, 25).

Cell size Of HOG	Image size		
	512×512	256×256	128×128
8 × 8	97.7	98.2	98.9
16 × 16	97.9	98.5	96.2
32 × 32	98.6	96.1	98.6

Table 4.23. ANN sensitivity results in percentage (50, 25, 25).

Cell size Of HOG	Image size		
	512×512	256×256	128×128
8 × 8	95.98	96.36	96.96
16 × 16	96.64	96.69	91.65
32 × 32	96.69	95.96	96.82

Table 4.24. ANN specificity results in percentage (50, 25, 25).

Cell size Of HOG	Image size		
	512×512	256×256	128×128
8 × 8	96.17	96.42	98.20
16 × 16	94.91	97.17	90.50
32 × 32	96.65	89.38	93.57

3) When the percentage of ANN (80% Training, 10%Validation, and 10% Testing) as illustrated in fpllowing tables [(4.25), (4.26), and (4.27)].

Table (4.25). ANN accuracy results in percentage (80, 10, 10).

Cell size Of HOG	Image size		
	512×512	256×256	128×128
8 × 8	99.7	99.3	99.4
16 × 16	99.6	99.4	99.5
32 × 32	99.5	98.7	99.5

Table 4.26. ANN sensitivity results in percentage (80, 10, 10).

Cell size Of HOG	Image size		
	512×512	256×256	128×128
8 × 8	98.73	98.72	99.32
16 × 16	99.36	98.63	98.73
32 × 32	98.63	98.10	99.37

Table 4.27. ANN specificity results in percentage (80, 10, 10).

Cell size Of HOG	Image size		
	512×512	256×256	128×128
8 × 8	96.50	97.92	98.05
16 × 16	97.22	96.75	98.33
32 × 32	96.67	94.37	95.75

A neural network pattern recognition tool is employed in ANN Classifier, where tumor and non-tumor features are fed into the network as input, while also specifying target groups. The best accuracy is obtained when 80% of the data is used for training, while 10% is used for network validation and testing. The network consists of 142884 input neurons

(number of features that are used in the classification process) and 180 neurons have been set as the maximum number in the hidden layer. The back-propagation function with Bayesian regularization was used to train the network. The neural network's accuracy and errors change as the network is retrained.

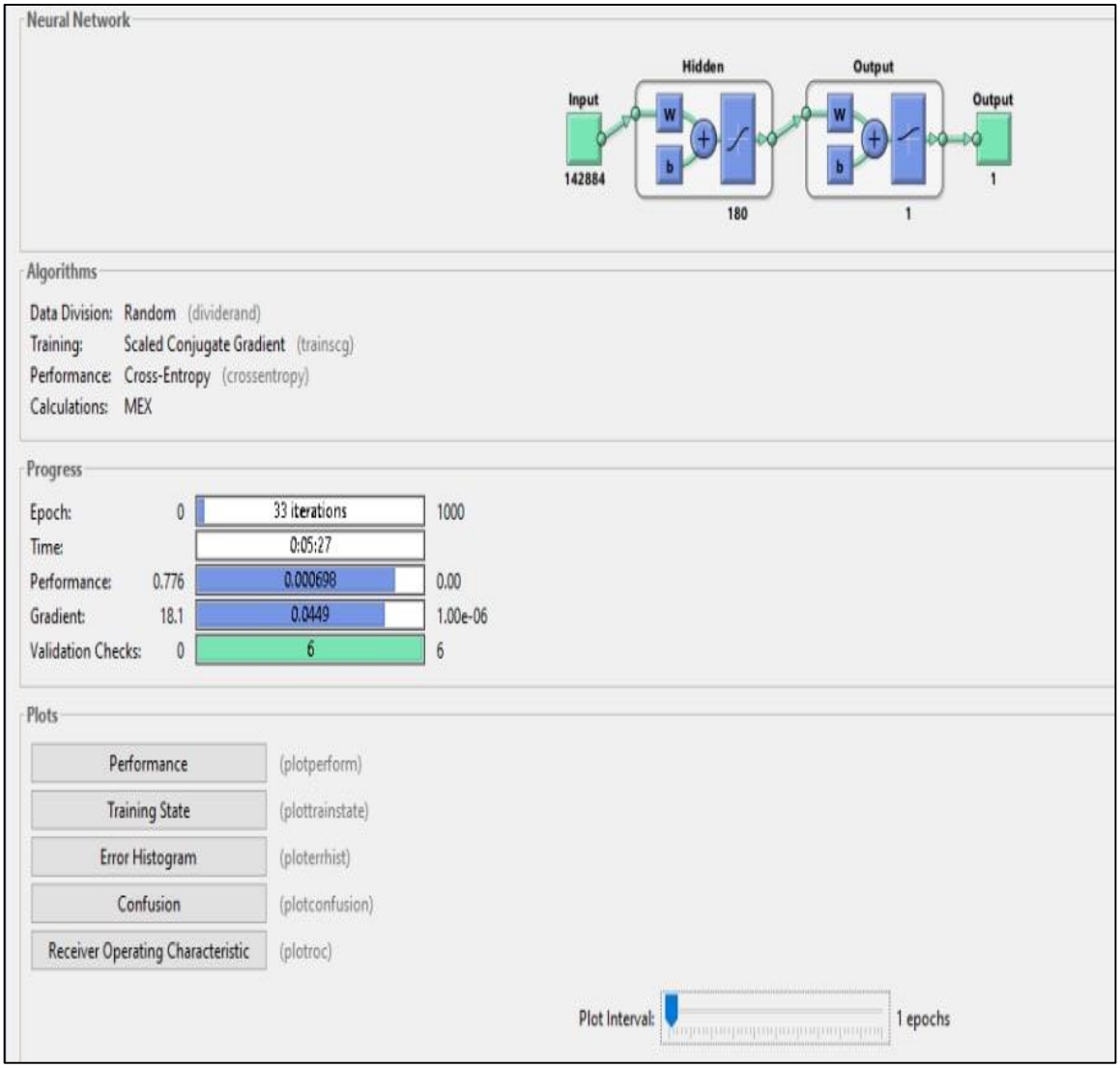

Figure 4.4. Artificial Neural Network Architecture& Training Parameters.

The Matlab tool is used to create an ANN confusion matrix, as shown in figure (4.5), A total of 1496 of the 1502 non-tumor MR images are correctly identified as belonging to the non-tumor target group, while the remaining 6 non-tumor images are misclassified as belonging to the tumor class target group. In 1498 tumor MR images, 1494 of the target classes

are correctly identified as being tumor, whereas 4 of the target classes are misidentified. ANN achieves an overall accuracy of 99.7% when the cell size of image is [512 512] and cell size of HOG is [8 8].

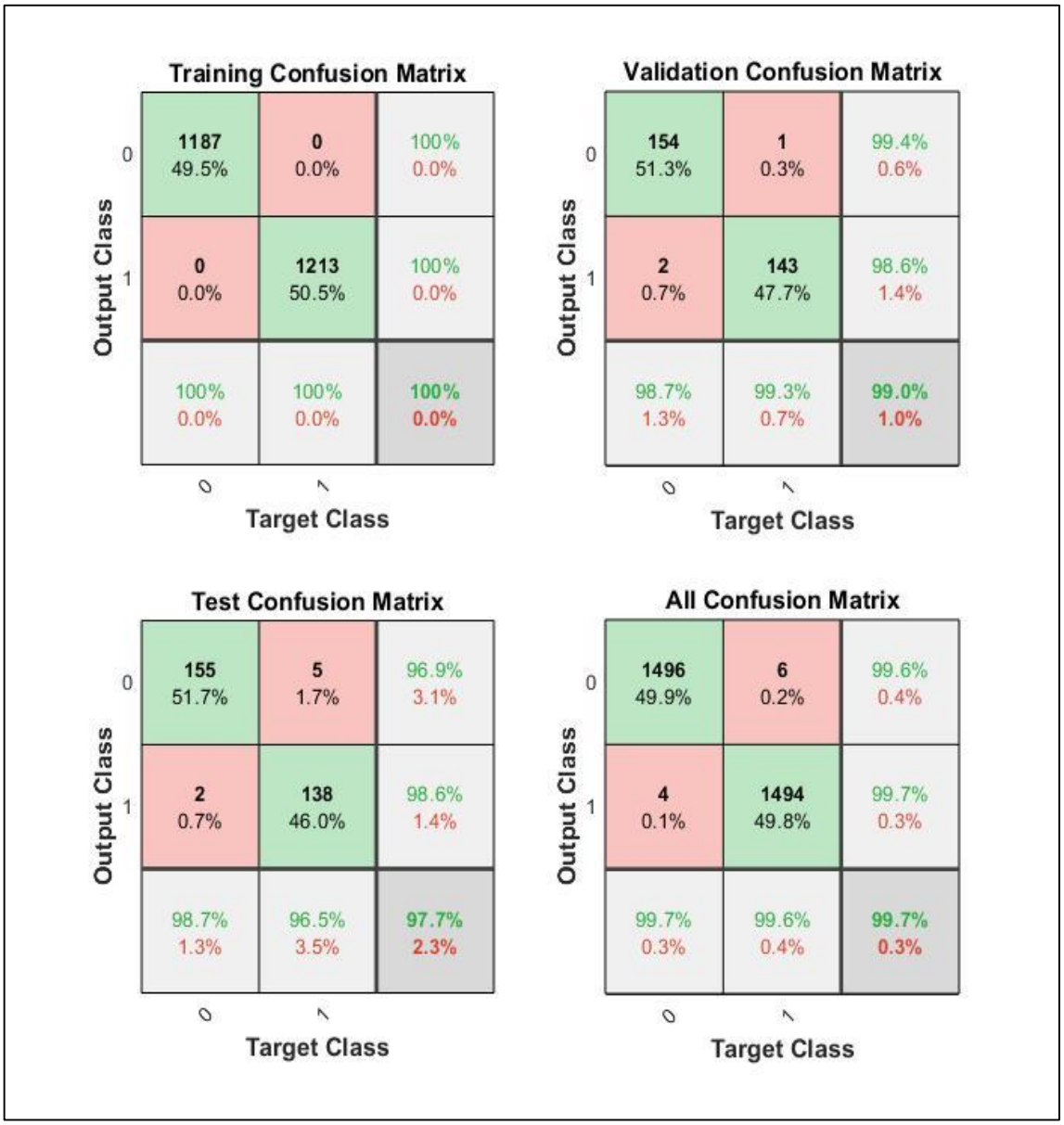

Figure 4.5. ANN confusion matrix with training, validation, and testing rate (80,10,10%)

Figure (4.6) depicts the Receiver's operational characteristics (ROC) of the machine learning algorithm for ANN to correctly recognize brain tumors. The relationship between the false-positive and true-positive rates is

represented by the ROC curve. A portion of the ROC curve's area is also shown in this figures.

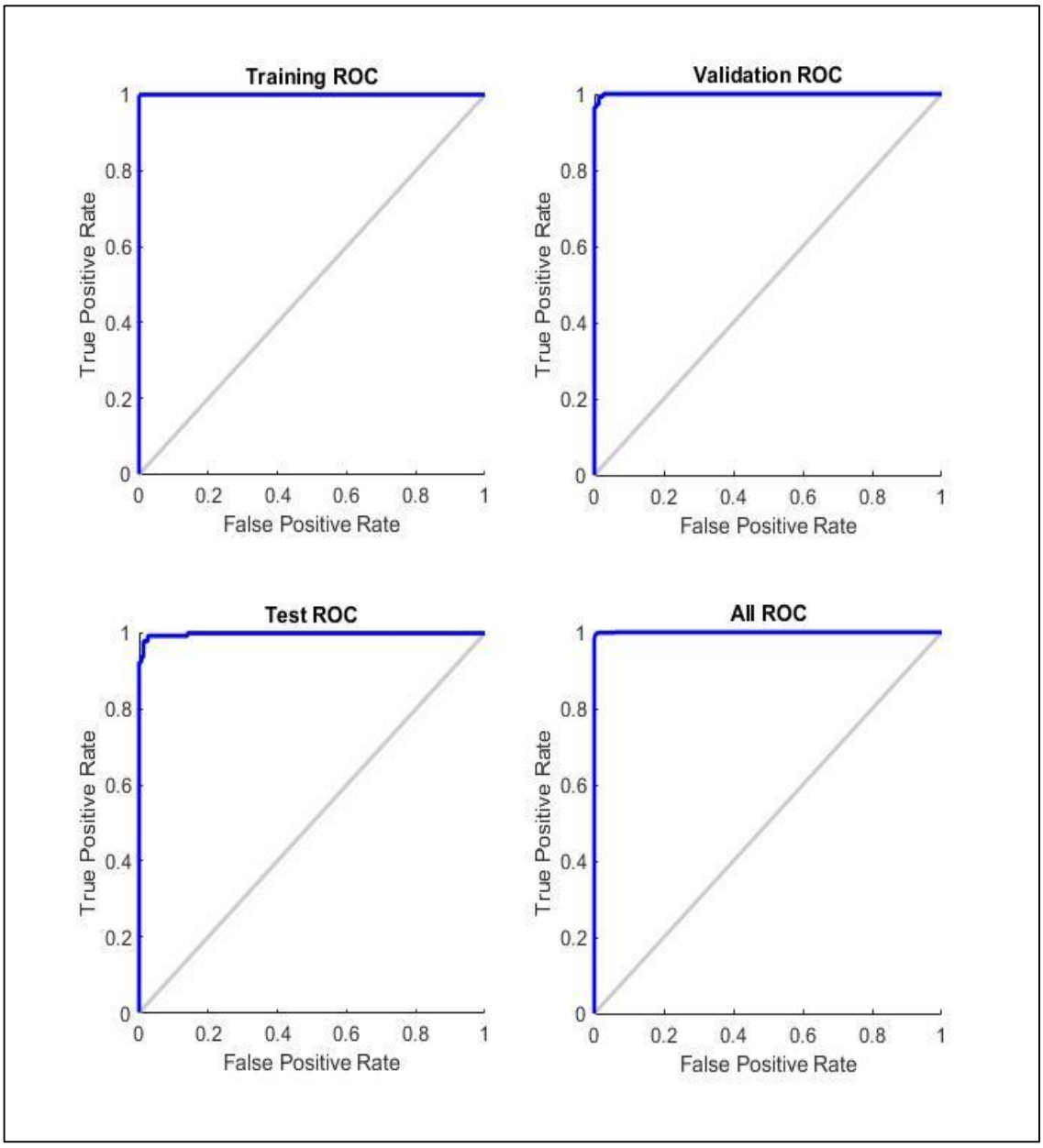

Figure 4.6. ROC curves for ANN model

When the network's performance on these validation vectors fails to advance the network's behavior or remains the same for a number of failed epochs, the training phase is terminated using the validation vectors. On the other hand, using the test vectors to determine whether the network is generalizing well has no impact on training. The validation checks are also shown in figure (4.7), which also depicts how the gradient is descending until it reaches the minimum at epoch 33.

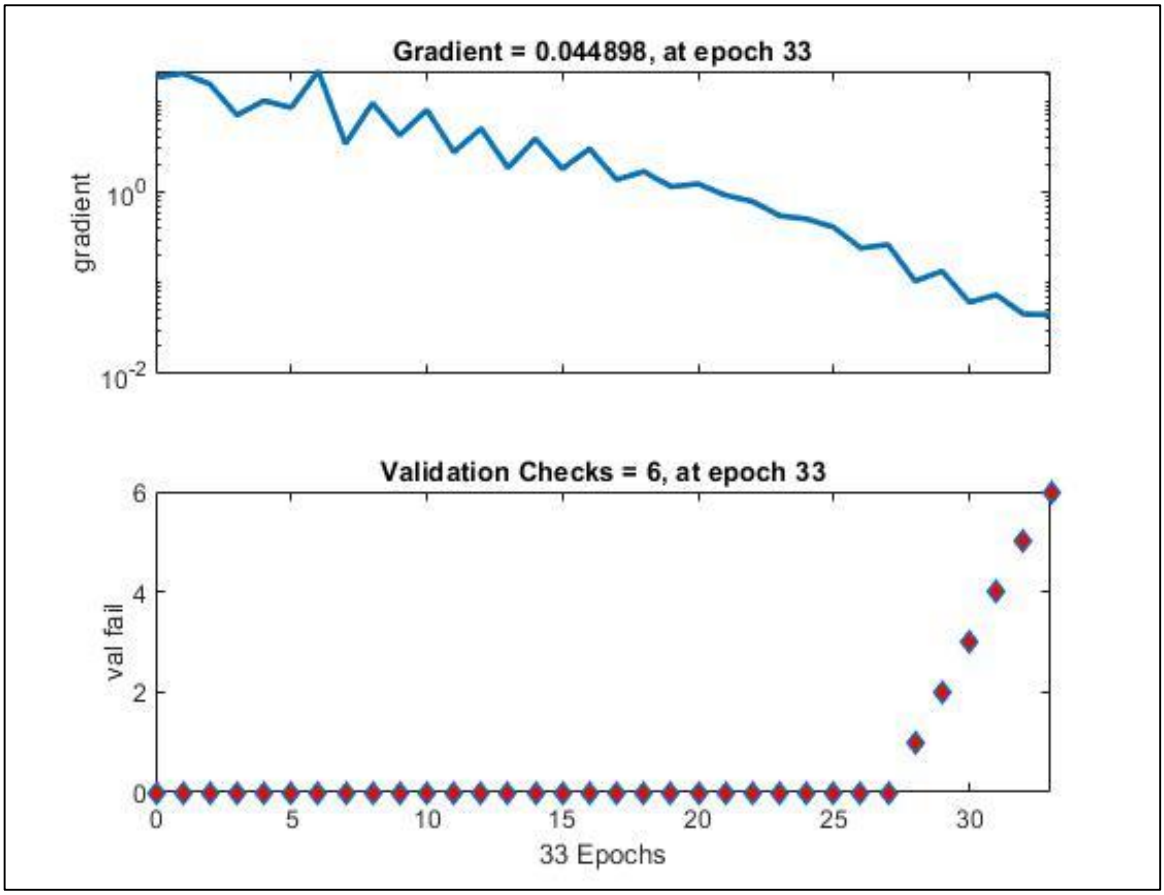

Figure 4.7. Training State of the network at 33 epochs

Figure (4.8) shows the best validation performance of ANN with the rate (80, 10, 10 %).

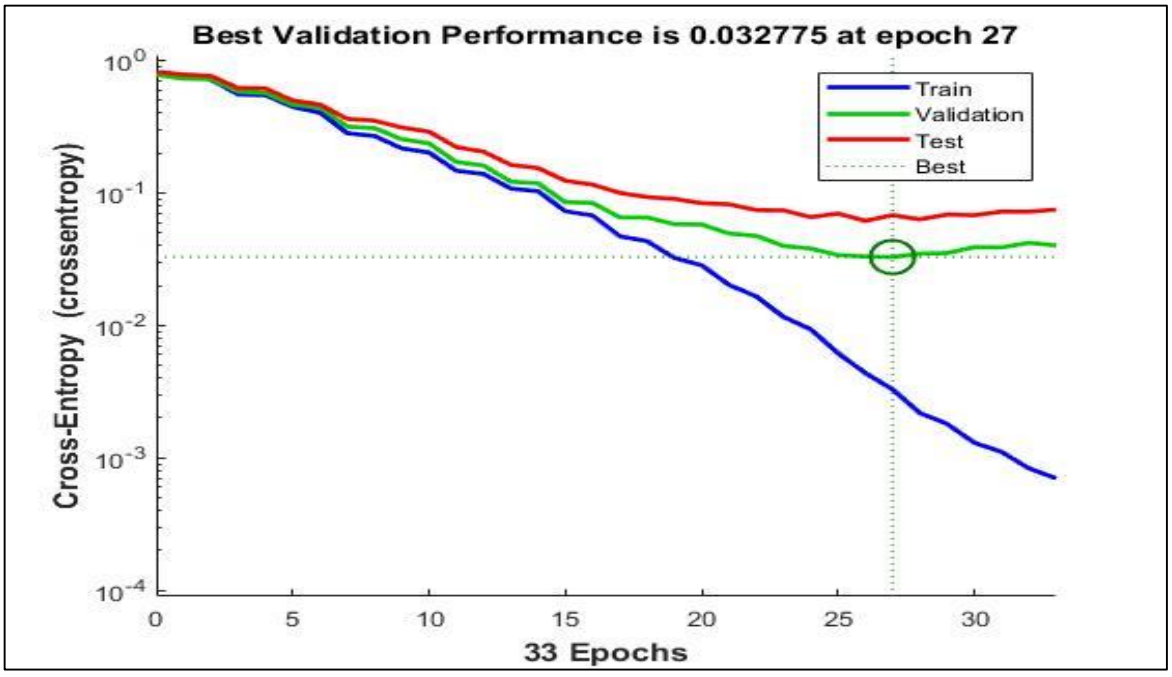

Figure 4.8. Network performance

The error histogram of the network throughout the training phase is also shown in figure 4.9.

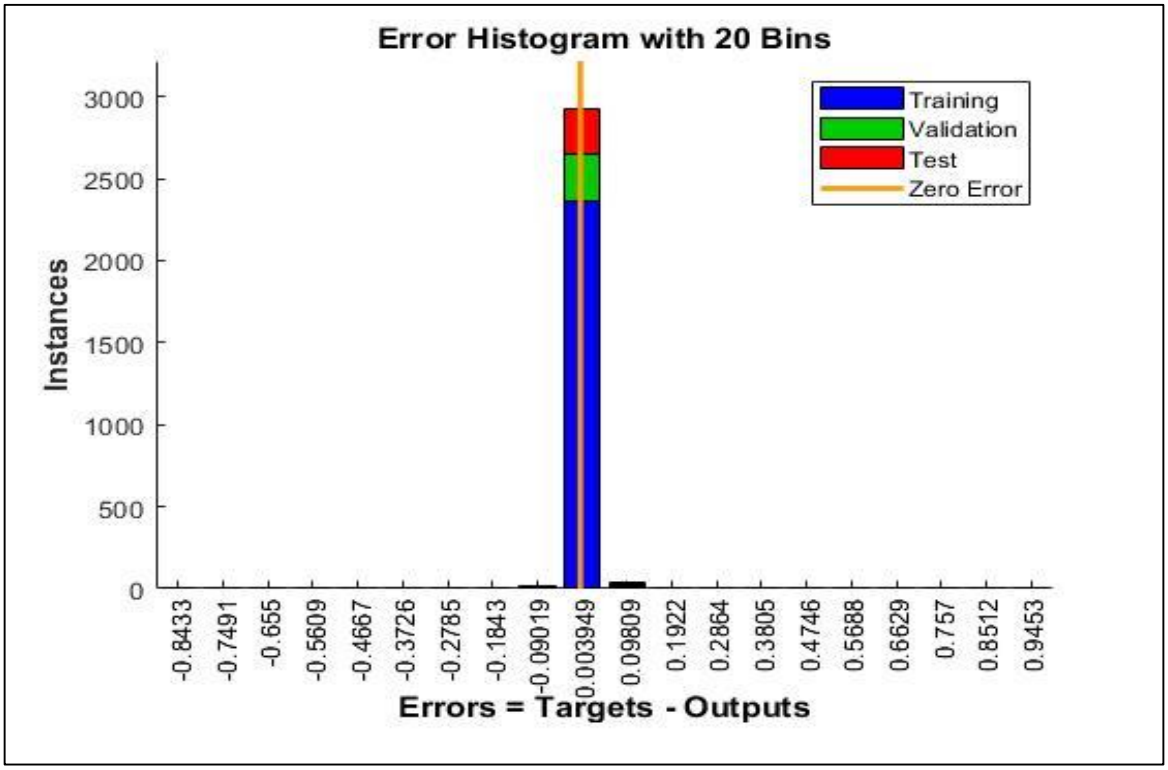

Figure 4.9. Error Histogram

4.3 Brain Tumor Segmentation Part:

The MRI image is filled with noise; to remove the noise, we applied a median filter with a window size of 5. K-Means clustering initially k centroid points are defined with k = 3. Thresholding was implemented with a global threshold to convert the grayscale image to binary. Morphological operations represented by erosion, dilation, opening, and closing were carried out on the binary image to remove the small objects from the thresholding step. In this algorithm, we utilized three types of structuring elements (disk shape with a radius of 5, square shape with a width of (3*3) pixels, and rectangular shape with a width of (3*9) pixels.

The F1score, Dice Coefficient (DC), and Jaccard Distance (JD) were performance assessment measures for segregating Brains MR images.

The findings of the suggested segmentation technique have been presented and associated quantitatively and qualitatively. Fig. (4.10) presents the segmentation process implemented utilizing the suggested method on four samples of brain slices (two HGG and two LGG images). The suggested segmentation process is applied in four stages: image preprocessing, K-mean clustering, thresholding, and morphological operations.

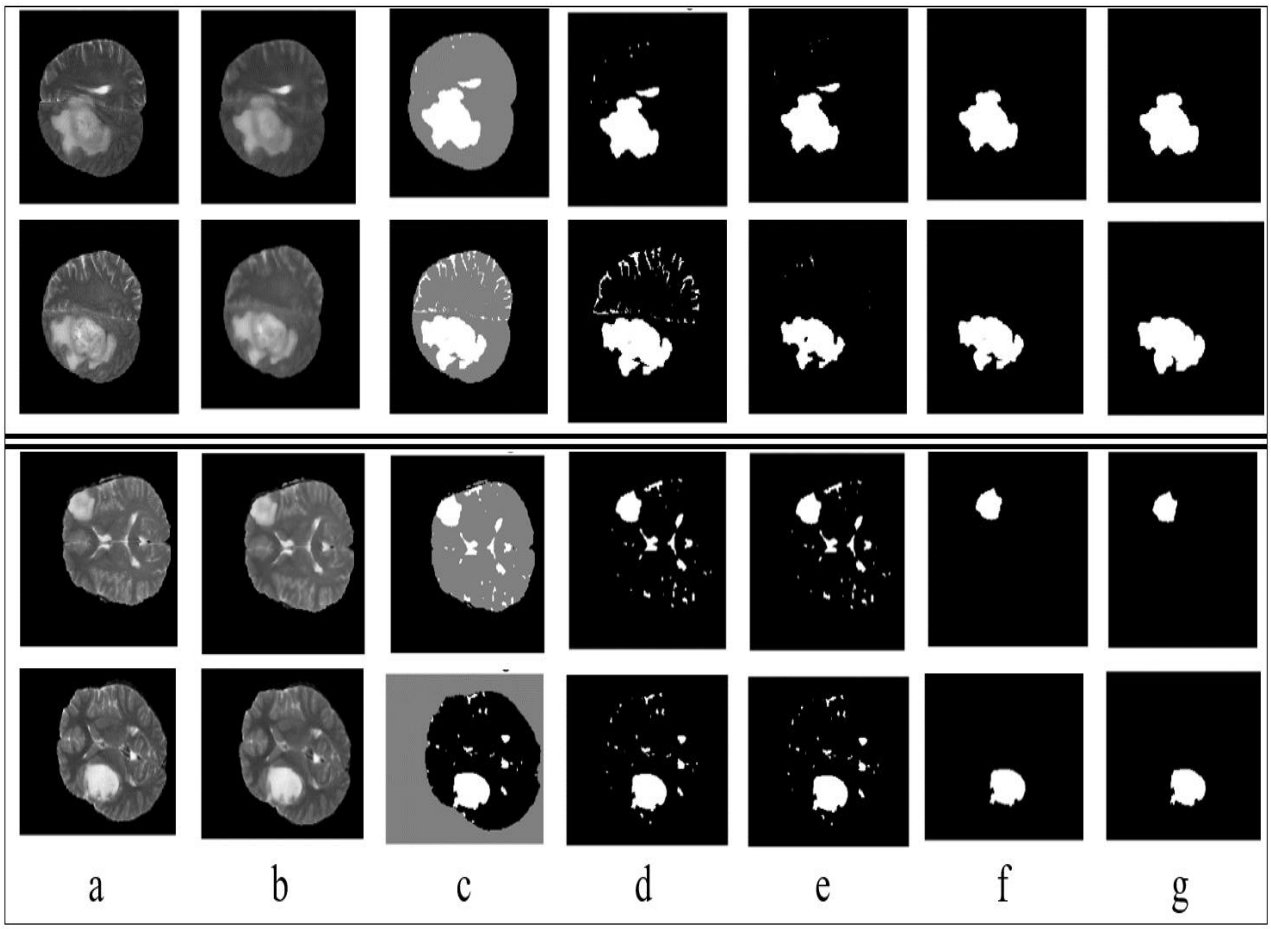

Figure 4.10. Segmentation process images, (a) original, (b) denoised, (c) k-means, (d) threshold, (e) eroded, (f) dilated, (g) segmented. (the upper two rows refer to the HGG images, while the lower two rows represent the LGG images).

figure 4.10(a) demonstrates an image with Gaussian noise, and the corresponding denoised image obtained utilizing median filtering is presented in figure 4.10 (b). To improve the stability of the segmentation algorithm. figure 4.10 (c) and 4.10 (d) exhibit the results of K-means and thresholding, respectively. It can be seen from figure 4.10 (d) the non-small

tumor regions. Four morphological operations are carried out to remove these non-tumor regions and fill the gaps in tumor images with disk shape structuring elements as demonstrated in the resulting images depicted in figure 4.10 (g).

To explore the influence of the structuring element on the segmentation process performance, three types are considered in this method, disk shape with a radius of 5, square shape with a width of (3*3) pixels, and rectangular shape with a width of (3*9) pixels. the results of a comparison between these three categories in terms of Dice are demonstrated in figure 4.11.

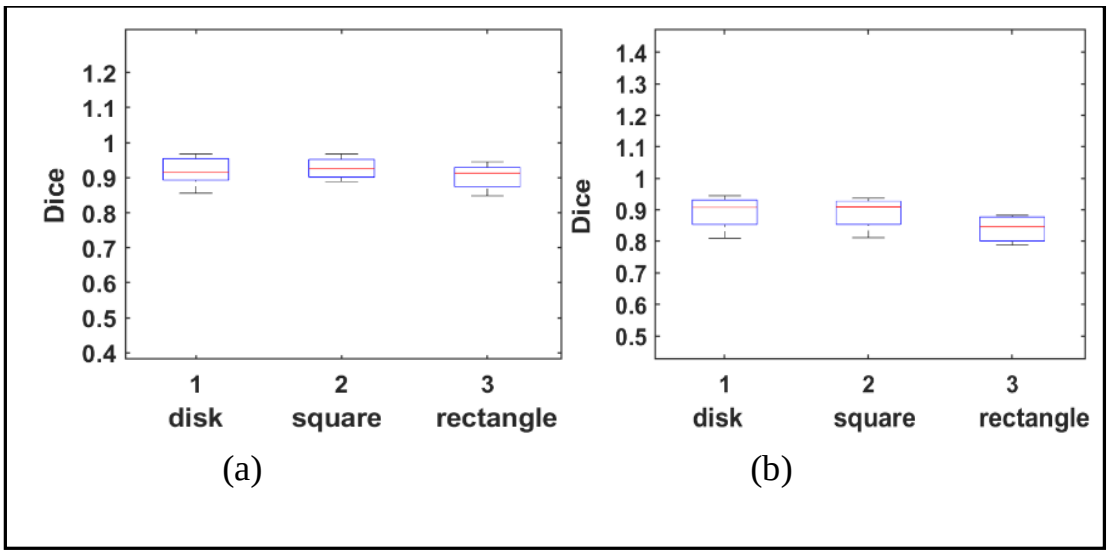

Figure 4.11. Performance of three structure element (disk, square, and rectangular) shapes in terms of Dice on (a) HGG and (b) LGG images.

Changes in the shape and size of the structuring element can alter the opening and closing processes. Every corner of the image has a different shape for the opening process due to the diverse shapes of the structuring element. When it comes to the closure process, it is clear that the varying sizes of the structural elements impact the outcome. As observed, square shape is the best performance compared to disk and rectangular.

Introducing k-means clustering before thresholding enhances the segmentation performance due to the beneficial characteristic of this technique in pixel representation. The suggested algorithm performance has been compared with a similar algorithm that does not use the k-means clustering (method1) technique for two classes of MRI brain pictures (HGG and LGG). Figs. 4.12 presents a comparison between the method with k-means clustering and without it. The effectiveness of k-means clustering on the segmentation concerning dice coefficient is clear.

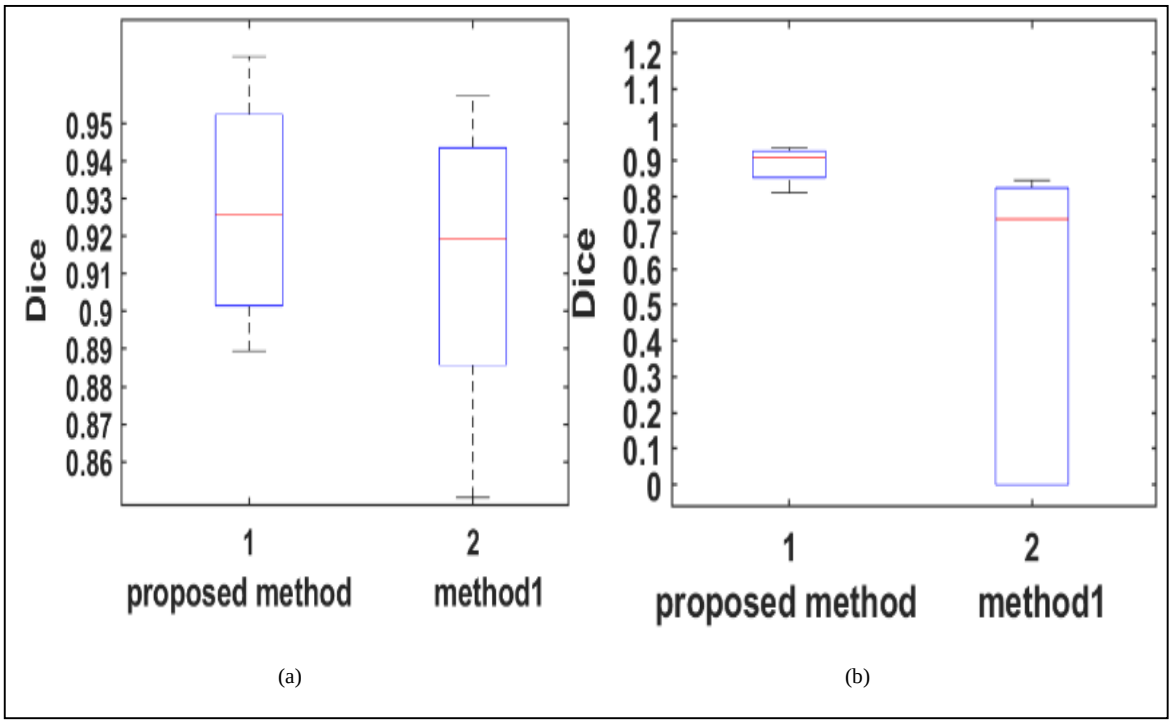

Figure 4.12. The differences between the suggested technique with and without clustering related to Dice applied to (a) HGG and (b) LGG images.

The median filter improves the segmentation process' performance by lowering the image's noise level and improving its aesthetic appearance.

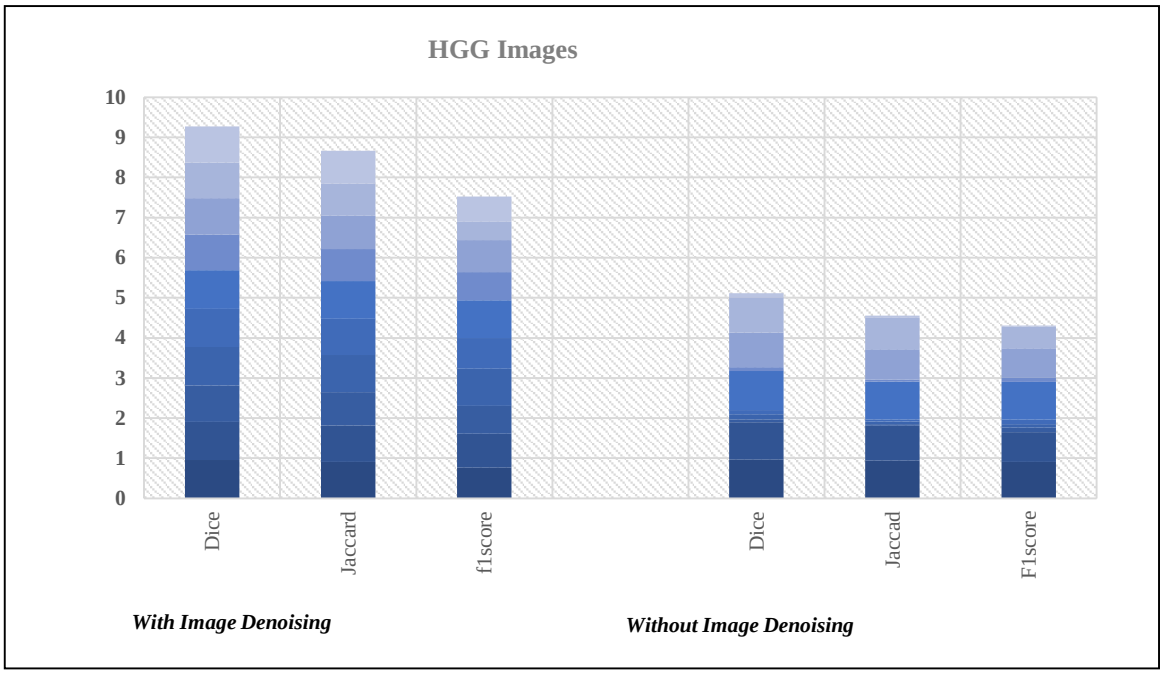

Figure 4.13. Performance of the Median filter on HGG Images.

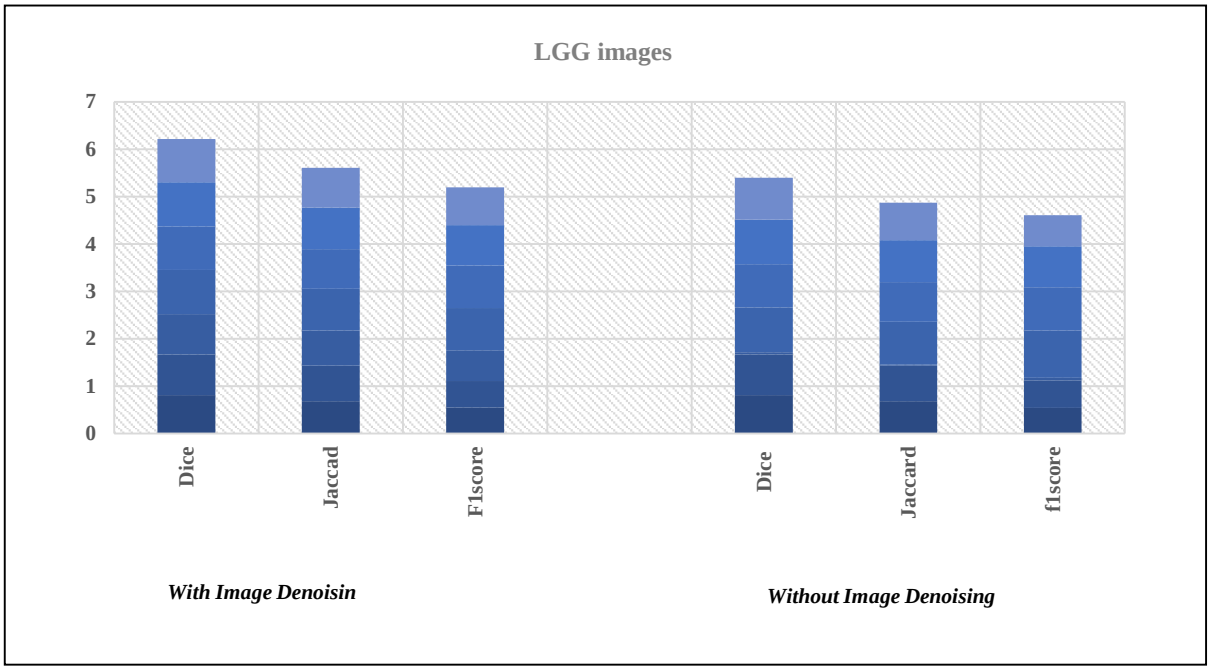

Figure 4.14. Performance of the Median filter on LGG Images

The results of comparing the method with and without the denoising process related to Dice, Jaccard, and F1 score were demonstrated in Figs. 4.11 and 4.12 for HGG and LGG images, respectively. Figures 4.13 and 4.14 demonstrate that utilizing image denoising in the preprocessing stage

improves performance compared to not utilizing the denoising procedure. Brains tumors segmentation is a significant stage in brain imaging diagnosis. As a result, it attracted many researchers in this subject. A comparison is undertaken for this aim, as demonstrated in Table 4.28, to assess the efficacy of the suggested method concerning past efforts utilizing the same brain images (BRATS). The results of our new method are better than the old one in terms of the Dice coefficient, as demonstrated in Table 4.28. The suggested method's impressive performance is due to a hybrid combination of k-means clustering, thresholding, and morphological operations (erosion, dilation, opening, and closing operations).

Table.4. 28. Performance comparisons between the state-of-the-art methods and suggested algorithm

Methods	**Dice Coefficient**	
	LGG	**HGG**
Bauer , et al.[59]	0.49	0.74
N. J. Tustison , et al.[60]	0.87	0.34
Pereira , et al.[61]	0.65	0.88
Soleymanifard & Hamghalam [62]	0.8627	0.8872
Ismael [19]	0.869	0.913
Suggested method	0.9368	0.9679

Chapter Five

Conclusion and Future Work

Chapter Five

Conclusion and Future Work

5.1.Conclusion:

For the patient to receive the best care, an accurate brain diagnosis is essential. Although it is an invasive procedure, the needle biopsy confirms the tumor's diagnosis. Additionally, the radiologist's visual analysis-based tumor diagnosis is laborious, arbitrary, and unreliable. Therefore, it is crucial to identify and segment brain MRI in order to help the radiologist make a quick and accurate tumor diagnosis. However, the currently used techniques fall short of the automation, accuracy, and efficiency needed in the medical field. This thesis research is therefore focused on improving the detection and segmentation of brain tumor MRI. The thesis work is divided into two sets detection part and segmentation part of brain tumors in MRI. **The first** section of this thesis's contributions focuses on a tumor classification scheme that is both accurate and effective for determining whether a brain MRI shows a tumor or not. The proposed method employs features of the brain, like HOG, to represent the properties of the brain. The feature extraction method, which was created for the detection and classification of tumors from brain MRI images, was tested in a variety of experimental scenarios using a collection of brain MRI datasets. Experimental outcomes demonstrated that our classification method can effectively distinguish between typical and abnormal brain MRI images. In this thesis, the effectiveness of machine learning algorithms for brain tumor detection is examined. Algorithms for classification were applied to the data set produced by using tissue-based characteristics of MR images. Utilizing the suggested three classifiers enhances the tumor classification's efficiency even more: (SVM), (ANN), and (k-NN). The image's characteristics were

assessed in accordance with the accuracy, specificity, and sensitivity findings from the confusion metrics using tenfold cross-validation. To train the features in the ANN model, three different ratios (testing, validation, and training) were applied. With the least amount of error and only one neuron in the hidden layers, the ratio (80%, 10%, 10%) produced the best result of 99.7% test accuracy. According to the findings presented in chapter four, ANN using this ratio and the HOG feature extraction process have higher classification accuracy than some of the more traditional existing methods.

The second part is a new automated brain tumor segmentation algorithm suggested in this thesis. This algorithm consists of a hybrid model that combines k-means clustering and thresholding techniques. A median filter was employed for noise reduction and image enhancement; on the other hand, morphological operations were carried out to improve the segmentation accuracy. This method was validated on MRI brain images obtained from BRATS datasets. Simulated findings demonstrate the powerful effectiveness and performance of the suggested system. In addition, k-means clustering is a beneficial segmentation technique, especially when applied with thresholding. Furthermore, image denoising empowers the algorithm's Dice, Jaccard, and F1 score performance. Utilizing the same MRI images, the approach suggested in this thesis outperforms existing methods. Even with many slices, it can help the radiologist analyze and diagnose MRI tumor images.

The results obtained from the simulation demonstrated the powerful achievements of the suggested algorithm in terms of accuracy was 99.7%, sensitivity was 99.4%, specificity was 99.5%, Dice ware 93.68% for LGG and 96.79% for HGG, Jaccard was 93.6, and F1 score was 96.8.

5.2.A future study:

To increase the accuracy of the classification, examine and quantify the features that can be extracted from other imaging modalities (like magnetic resonance spectroscopy and ultrasonography) and combine them with the features used in the current work.

1. The generalization capacity of the proposed classification scheme is anticipated to be further enhanced by more extensive training utilizing larger datasets for machine learning or deep learning.
2. Since SVM classifies tumors sequentially, it is possible to parallelize these classifications to increase classification effectiveness.
3. Local binary pattern and log Gabor algorithms can be used to extract the features of images as opposed to the HOG.
4. The proposed algorithm can be tested on various MRI databases or on actual MRI scans before being improved with various tumor types.

References

References

[1] M. Pichaivel, G. Anbumani, P. Theivendren, and M. Gopal, “An Overview of Brain Tumor,” in *Brain Tumors*, IntechOpen, 2022.

[2] S. Bauer, R. Wiest, L.-P. Nolte, and M. Reyes, “A survey of MRI-based medical image analysis for brain tumor studies,” *Phys. Med. Biol.*, vol. 58, no. 13, pp. R97–R129, Jul. 2013.

[3] D. Ricard, A. Idbaih, F. Ducray, M. Lahutte, K. Hoang-Xuan, and J.-Y. Delattre, “Primary brain tumours in adults,” *Lancet*, vol. 379, no. 9830, pp. 1984–1996, May 2012.

[4] M. Havaei, H. Larochelle, P. Poulin, and P.-M. Jodoin, “Within-brain classification for brain tumor segmentation,” *Int. J. Comput. Assist. Radiol. Surg.*, vol. 11, no. 5, pp. 777–788, May 2016.

[5] M. Gurbina, M. Lascu, and D. Lascu, “Tumor detection and classification of MRI brain image using different wavelet transforms and support vector machines,” *2019 42nd International Conference on Telecommunications and Signal Processing, TSP 2019*. pp. 505–508, 2019.

[6] Sharma Komal, Kaur Akwinder, and Gujral Shruti, “Brain tumor detection Using Machine learning Algorithms.” pp. 15–20, 2014.

[7] S. . Olabarriaga and A. W. . Smeulders, “Interaction in the segmentation of medical images: A survey,” *Med. Image Anal.*, vol. 5, no. 2, pp. 127–142, Jun. 2001.

[8] T. S. Deepthi Murthy and G. Sadashivappa, “Brain tumor segmentation using thresholding, morphological operations and extraction of features of tumor,” in *2014 International Conference on Advances in Electronics Computers and Communications*, Oct. 2014, pp. 1–6.

[9] H. Hooda, O. P. Verma, and T. Singhal, “Brain tumor segmentation: A performance analysis using K-Means, Fuzzy C-Means and Region growing algorithm,” *Proceedings of 2014 IEEE International Conference on Advanced Communication, Control and Computing Technologies, ICACCCT 2014*. pp. 1621–1626, 2015.

[10] N. Gordillo, E. Montseny, and P. Sobrevilla, “State of the art survey on MRI brain tumor segmentation,” *Magn. Reson. Imaging*, vol. 31, no. 8, pp. 1426–1438, Oct. 2013.

[11] A. A. Padmanabha G, S. Y. Pattar, and A. Professor, “Textural Feature Extraction and Analysis for Brain Tumors using MRI,” *International Journal of Scientific and Research Publications*, vol. 7, no. 8. pp. 185–

190, 2017, [Online]. Available: www.ijsrp.org.

[12] M. R. Islam, M. R. Imteaz, and Marium-E-Jannat, "Detection and analysis of brain tumor from MRI by Integrated Thresholding and Morphological Process with Histogram based method," *International Conference on Computer, Communication, Chemical, Material and Electronic Engineering, IC4ME2 2018*. 2018.

[13] D. Reddy, Dheeraj, Kiran, V. Bhavana, and H. . Krishnappa, "Brain Tumor Detection Using Image Segmentation Techniques," in *2018 International Conference on Communication and Signal Processing (ICCSP)*, Apr. 2018, pp. 0018–0022.

[14] A. Wadhwa, A. Bhardwaj, and V. Singh Verma, "A review on brain tumor segmentation of MRI images," *Magn. Reson. Imaging*, vol. 61, pp. 247–259, Sep. 2019.

[15] M. Gurbina, M. Lascu, and D. Lascu, "Tumor Detection and Classification of MRI Brain Image using Different Wavelet Transforms and Support Vector Machines," in *2019 42nd International Conference on Telecommunications and Signal Processing (TSP)*, Jul. 2019, pp. 505–508.

[16] C. Zhang, X. Shen, H. Cheng, and Q. Qian, "Brain Tumor Segmentation Based on Hybrid Clustering and Morphological Operations," *Int. J. Biomed. Imaging*, vol. 2019, pp. 1–11, Apr. 2019.

[17] J. Amin, M. Sharif, M. Yasmin, and S. L. Fernandes, "A distinctive approach in brain tumor detection and classification using MRI," *Pattern Recognit. Lett.*, vol. 139, pp. 118–127, Nov. 2020.

[18] T. Saba, A. Sameh Mohamed, M. El-Affendi, J. Amin, and M. Sharif, "Brain tumor detection using fusion of hand crafted and deep learning features," *Cogn. Syst. Res.*, vol. 59, pp. 221–230, Jan. 2020.

[19] M. Rashid Ismael, "Edge Enhancement Based Active Contour Model for Segmentation of Brain Tumor in MRI Images," *ECTI Trans. Electr. Eng. Electron. Commun.*, vol. 19, no. 3, Sep. 202.

[20] S. Deepak and P. M. Ameer, "Automated Categorization of Brain Tumor from MRI Using CNN features and SVM," *J. Ambient Intell. Humaniz. Comput.*, vol. 12, no. 8, pp. 8357–8369, Aug. 202.

[21] R. Mostafiz, M. S. Uddin, N.-A. Alam, M. M. Hasan, and M. M. Rahman, "MRI-based brain tumor detection using the fusion of histogram oriented gradients and neural features," *Evol. Intell.*, vol. 14, no. 2, pp. 1075–1087, Jun. 2021.

[22] D. M. Toufiq, A. M. Sagheer, and H. Veisi, “Brain Tumor Segmentation from Magnetic Resonance Image using Optimized Thresholded Difference Algorithm and Rough Set,” *TEM J.*, pp. 631–638, May 2022.

[23] H. Habib, R. Amin, B. Ahmed, and A. Hannan, “Hybrid algorithms for brain tumor segmentation, classification and feature extraction,” *J. Ambient Intell. Humaniz. Comput.*, vol. 13, no. 5, pp. 2763–2784, May 2022.

[24] S. Rinesh *et al.*, “Investigations on Brain Tumor Classification Using Hybrid Machine Learning Algorithms,” *J. Healthc. Eng.*, vol. 2022, pp. 1–9, Feb. 2022.

[25] M. T. Nyo, F. Mebarek-Oudina, S. S. Hlaing, and N. A. Khan, “Otsu’s thresholding technique for MRI image brain tumor segmentation,” *Multimed. Tools Appl.*, May 2022.

[26] A. Işın, C. Direkoğlu, and M. Şah, “Review of MRI-based Brain Tumor Image Segmentation Using Deep Learning Methods,” *Procedia Comput. Sci.*, vol. 102, pp. 317–324, 2016.

[27] O. S. Kareem, A. K. AL-Sulaifanie, D. A. Hasan, and D. M. Ahmed, “Segmenting and Classifiying the Brain Tumor from MRI Medical Images Based on Machine Learning Algorithms: A Review,” *Asian J. Res. Comput. Sci.*, pp. 50–61, Jul. 202.

[28] “Localization and Classification of Brain Tumor using Machine Learning & Deep Learning Techniques,” *Int. J. Innov. Technol. Explor. Eng.*, vol. 8, no. 9S, pp. 59–66, Aug. 2019.

[29] L. P. Kaelbling, M. L. Littman, and A. W. Moore, “Reinforcement Learning: A Survey,” *J. Artif. Intell. Res.*, vol. 4, pp. 237–285, May 1996.

[30] A. Gokulalakshmi, S. Karthik, N. Karthikeyan, and M. S. Kavitha, “ICM-BTD: improved classification model for brain tumor diagnosis using discrete wavelet transform-based feature extraction and SVM classifier,” *Soft Computing*, vol. 24, no. 24. pp. 18599–18609, 2020.

[31] M. S. S. Hunnur, A. Raut, and S. Kulkarni, “Implementation of image processing for detection of brain tumors,” *Proceedings of the International Conference on Computing Methodologies and Communication, ICCMC 2017*, vol. 2018-Janua. pp. 717–722, 2018.

[32] K. Umamaheswari, P. Rajesh, S. S. Rao, and P. V. Babu, “Application of Segmentation Methodology for Extracting MRI Brain Tumor Duly Mitigating the Noise,” *Proceedings - 2015 International Conference*

on Computational Intelligence and Communication Networks, CICN 2015. pp. 288–292, 2016.

[33] C. Zhang, X. Shen, H. Cheng, and Q. Qian, "Brain tumor segmentation based on hybrid clustering and morphological operations," *International Journal of Biomedical Imaging*, vol. 2019. 2019.

[34] H. M. Al-Dabbas and A. H. Morad, "Medical Image Enhancement to Extract Brain Tumors from CT and MRI images," *Iraqi J. Sci.*, pp. 1820–1829, Aug. 2019.

[35] A. Kharrat, M. Ben Halima, and M. Ben Ayed, "MRI brain tumor classification using Support Vector Machines and meta-heuristic method," *International Conference on Intelligent Systems Design and Applications, ISDA*, vol. 2016-June. pp. 446–451, 2016.

[36] Zahoor Ahmad, "Brain Tumor Detection Features Extraction From MR Images Using Segmentation, Image Optimization Classification Techniques," *International Journal of Engineering Research and*, vol. V7, no. 10. 2018.

[37] "Texture Feature Extraction and Classification of Brain Neoplasm in MR Images using Machine Learning Techniques," *Int. J. Recent Technol. Eng.*, vol. 8, no. 5, pp. 2319–2325, Jan. 2020.

[38] P. K* and M. V Karki, "Texture Feature Extraction and Classification of Brain Neoplasm in MR Images using Machine Learning Techniques," *Int. J. Recent Technol. Eng.*, vol. 8, no. 5, pp. 2319–2325, Jan. 2020.

[39] S. Wei, S. Zou, F. Liao, and W. Lang, "A Comparison on Data Augmentation Methods Based on Deep Learning for Audio Classification," *J. Phys. Conf. Ser.*, vol. 1453, no. 1, 2020.

[40] R. C. Gonzalez and R. E. Woods, "4TH EDITION Digital image processing." p. 1168, 2018.

[41] B. Abd Alreda, H. Khalif, and T. Saeid, "Automated Brain Tumor Detection Based on Feature Extraction from The MRI Brain Image Analysis," *Iraqi J. Electr. Electron. Eng.*, vol. 16, no. 2, pp. 1–10, Dec. 2020.

[42] K. Mridha, A. P. Pandey, A. Ranpariya, A. Ghosh, and R. N. Shaw, "Web Based Brain Tumor Detection using Neural Network," *2021 IEEE 6th International Conference on Computing, Communication and Automation, ICCCA 2021*. pp. 137–143, 2021.

[43] M. D. Steenwijk *et al.*, "Accurate white matter lesion segmentation by

k nearest neighbor classification with tissue type priors (kNN-TTPs)," *NeuroImage Clin.*, vol. 3, pp. 462–469, 2013.

[44] A. Hussain and A. Khunteta, "Semantic Segmentation of Brain Tumor from MRI Images and SVM Classification using GLCM Features," in *2020 Second International Conference on Inventive Research in Computing Applications (ICIRCA)*, Jul. 2020, pp. 38–43.

[45] G. B. Gebrea, T. Urgessab, and T.GopiKrishna, "Artificial Neural Network Based Amharic Language Speaker Recognition," *Turkish J. Comput. Math. Educ.*, vol. 12, no. 3, pp. 5105–5116, 2021.

[46] M. SABER, A. EL RHARRAS, R. SAADANE, H. KHARRAZ AROUSSI, and M. WAHBI, "Artificial Neural Networks, Support Vector Machine And Energy Detection For Spectrum Sensing Based On Real Signals," *Int. J. Commun. Networks Inf. Secur.*, vol. 11, no. 1, Apr. 2022.

[47] M. Dawngliana, D. Deb, M. Handique, and S. Roy, "Automatic brain tumor segmentation in MRI: Hybridized multilevel thresholding and level set," *2015 International Symposium on Advanced Computing and Communication, ISACC 2015*. pp. 219–223, 2016.

[48] M. O. Khairandish, M. Sharma, V. Jain, J. M. Chatterjee, and N. Z. Jhanjhi, "A Hybrid CNN-SVM Threshold Segmentation Approach for Tumor Detection and Classification of MRI Brain Images," *IRBM*, Jun. 2021.

[49] Y. Sharma and Y. K. Meghrajani, "Brain tumor extraction from MRI image using mathematical morphological reconstruction," *Proceedings on 2014 2nd International Conference on "Emerging Technology Trends in Electronics, Communication and Networking", ET2ECN 2014*. 2015.

[50] J. Fenshia Singh and V. Magudeeswaran, "Thresholding based method for segmentation of MRI brain images," *Proceedings of the International Conference on IoT in Social, Mobile, Analytics and Cloud, I-SMAC 2017*. pp. 280–283, 2017.

[51] J. Rani, R. Kumar, F. A. Talukdar, and N. Dey, "The Brain Tumor Segmentation Using Fuzzy C-Means Technique," in *Computer Vision*, IGI Global, 2018, pp. 2402–2419.

[52] S. Saritha and N. Amutha Prabha, "A comprehensive review: Segmentation of MRI images-brain tumor," *Int. J. Imaging Syst. Technol.*, vol. 26, no. 4, pp. 295–304, Dec. 2016.

[53] A. Hazra, A. Dey, S. K. Gupta, and M. A. Ansari, "Brain tumor

detection based on segmentation using MATLAB," *2017 International Conference on Energy, Communication, Data Analytics and Soft Computing, ICECDS 2017*. pp. 425–430, 2018.

[54] N. A. Kamal R, "Brain Tumor Detection and Identification Using K-Means Clustering Technique," *Special Issue Published in Int. Jnl. Of Advanced Networking and Applications*. 2015.

[55] M. A. Ansari, R. Mehrotra, and R. Agrawal, "Detection and classification of brain tumor in MRI images using wavelet transform and support vector machine," *Journal of Interdisciplinary Mathematics*, vol. 23, no. 5. pp. 955–966, 2020.

[56] S. Krishnakumar and K. Manivannan, "RETRACTED ARTICLE: Effective segmentation and classification of brain tumor using rough K means algorithm and multi kernel SVM in MR images," *J. Ambient Intell. Humaniz. Comput.*, vol. 12, no. 6, pp. 6751–6760, Jun. 2021.

[57] M. J. Lakshmi and S. N. Rao, "Effect of K-fold cross validation on Mri brain images using support vector machine algorithm," *International Journal of Recent Technology and Engineering*, vol. 7, no. 6. pp. 301–307, 2019.

[58] https://www.kaggle.com/datasets/ahmedhamada0/brain-tumor-detection.

[59] B. H. Menze *et al.*, "The Multimodal Brain Tumor Image Segmentation Benchmark (BRATS)," *IEEE Trans. Med. Imaging*, vol. 34, no. 10, pp. 1993–2024, Oct. 2015.

[60] N. J. Tustison *et al.*, "Optimal Symmetric Multimodal Templates and Concatenated Random Forests for Supervised Brain Tumor Segmentation (Simplified) with ANTsR," *Neuroinformatics*, vol. 13, no. 2. pp. 209–225, 2015.

[61] S. Pereira, A. Pinto, V. Alves, and C. A. Silva, "Brain Tumor Segmentation Using Convolutional Neural Networks in MRI Images," *IEEE Transactions on Medical Imaging*, vol. 35, no. 5. pp. 1240–1251, 2016.

[62] M. Soleymanifard and M. Hamghalam, "Segmentation of Whole Tumor Using Localized Active Contour and Trained Neural Network in Boundaries," in *2019 5th Conference on Knowledge Based Engineering and Innovation (KBEI)*, Feb. 2019, pp. 739–744.

الخلاصه

ورم الدماغ هو نمو غير طبيعي للخلايا داخل الدماغ. بعضها حميدة والبعض الآخر خبيث. يمكن أن تنمو الأورام من أنسجة المخ نفسها (الأولية) ، أو يمكن أن ينتشر السرطان من مكان آخر في الجسم إلى الدماغ (ورم خبيث). تعتبر أورام الدماغ من الأمراض القاتلة لأن معدل البقاء على قيد الحياة فيها منخفض جدا لذلك من أجل توفير علاج فعال يلزم إجراء تشخيص دقيق لهذه الأورام. يوفر التصوير بالرنين المغناطيسي (MRI) تفاصيل معلومات حول تشريح ورم الدماغ ، التركيب الخلوي وإمداد الأوعية الدموية ، مما يجعلها أداة مهمة للتشخيص الفعال والعلاج ومراقبة المرض.

الكشف الآلي عن ورم الدماغ من خلال صور التصوير بالرنين المغناطيسي هو من أصعب المهام في الطب الحديث. تتطلب التجزئه التلقائيه لصور الدماغ جهد اكبر ، وهي عملية تقسيم الصورة في مناطق متميزة ، هي واحدة من أكثر الجوانب المهمه. الضوضاء الموجودة في تصوير الدماغ بالرنين المغناطيسي الصور هي ضوضاء مضاعفة وتقليلها مهمة صعبة. لانه لايجب تدمير وازالة التفاصيل التشريحية الدقيقة للدماغ. فيجب العمل بدقه وحذر. لذا فان تجزئة صور الدماغ تعتبر تحديًا. لكنه جدا مهم وحاسم للتشخيص الدقيق. والتي تساعد أخصائي الأشعة في تشخيص الدماغ. يعد الكشف اليدوي وتجزئة منطقة الورم من شرائح التصوير بالرنين المغناطيسي عملية معقدة وتستغرق وقتًا طويلاً ، خاصة عند التعامل مع عدد كبير من صور التصوير بالرنين المغناطيسي. لذلك ، مطلوب نموذج كشف فعال وموثوق. في هذا العمل ، تم اقتراح طريقة التشخيص الآلي التي تتكون من خطوتين رئيسيتين ؛ الكشف عن شريحة الورم وتجزئة منطقة الورم في الشريحة المكتشفة. في خطوة الكشف ، استخدمنا التعلم الآلي لاكتشاف وتصنيف التصوير بالرنين المغناطيسي للدماغ ، ويتم استخراج الميزات من كل شريحة تصوير بالرنين المغناطيسي باستخدام الرسم البياني للتدرج الموجه (HOG)، ثم يتم تصنيف هذه الشرائح إلى صور الورم وغير الورمية باستخدام ثلاثة أنواع من نماذج المصنفات (KNN) و (SVM) و .(ANN) تم العثور على خوارزمية ANN بمعدل دقة 99.7٪ لتكون أفضل مقارنة بالخوارزميات الأخرى. من ناحية أخرى ، يتم تنفيذ طرق التجميع والعتبة والعمليات المورفولوجية في خطوة التجزئة. يستخدم المرشح المتوسط لتحسين جودة شرائح التصوير بالرنين المغناطيسي وتحسين أداء التجزئة عن طريق تقليل مستوى الضوضاء. أظهرت أربع عمليات مورفولوجية تحسينات كبيرة في عملية التجزئة ، والتعرية ، والتمدد ، والإغلاق ، والفتح. تم تنفيذ التجارب على مجموعتي بيانات ، Kaggle التي تتكون من (3000) صورة ، و BRATSصور عالية الجودة (HGG) وصورة منخفضة الدرجة .(LGG) أظهرت النتائج التي تم الحصول عليها من التجارب المحاكاة الإنجازات القوية للخوارزمية المقترحة من حيث الدقة

والحساسية والنوعية والنرد وجاكارد .ودرجة .F1 علاوة على ذلك ، تتفوق الطريقة المقترحة على بعض التقنيات الأخرى عند تطبيقها على نفس الصور.

جمهورية العراق
وزارة التعليم العالي والبحث العلمي
جامعة بابل
كلية الهندسة / قسم الهندسة الكهربائية

الكشف والتجزئة الالية لورم الدماغ بالاعتماد على صور الرنين المغناطيسي

رسالة

مقدمة الى كلية الهندسة في جامعة بابل

كجزء من متطلبات نيل درجة الماجستيرفي الهندسة

/الهندسه الكهربائية / الكترونيك صناعي

من قبل:

رشا تركي خلخال حسين اليساري

باشراف:

الدكتور مصطفى رشيد اسماعيل

1444هـ 2023م